EPRI | ELECTRIC POWER RESEARCH INSTITUTE

# Program on Technology Innovation: Research on Ammonium Bisulfate (ABS) Formation in Air Preheaters

*Experimental Investigation and Computational Fluid Dynamics (CFD) Modeling*

**1016164**

# Program on Technology Innovation: Research on Ammonium Bisulfate (ABS) Formation in Air Preheaters

*Experimental Investigation and Computational Fluid Dynamics (CFD) Modeling*

1016164

Technical Update, June 2008

EPRI Project Manager

J. Stallings

ELECTRIC POWER RESEARCH INSTITUTE
3420 Hillview Avenue, Palo Alto, California 94304-1338 ▪ PO Box 10412, Palo Alto, California 94303-0813 ▪ USA
800.313.3774 ▪ 650.855.2121 ▪ askepri@epri.com ▪ www.epri.com

## DISCLAIMER OF WARRANTIES AND LIMITATION OF LIABILITIES

THIS DOCUMENT WAS PREPARED BY THE ORGANIZATION(S) NAMED BELOW AS AN ACCOUNT OF WORK SPONSORED OR COSPONSORED BY THE ELECTRIC POWER RESEARCH INSTITUTE, INC. (EPRI). NEITHER EPRI, ANY MEMBER OF EPRI, ANY COSPONSOR, THE ORGANIZATION(S) BELOW, NOR ANY PERSON ACTING ON BEHALF OF ANY OF THEM:

(A) MAKES ANY WARRANTY OR REPRESENTATION WHATSOEVER, EXPRESS OR IMPLIED, (I) WITH RESPECT TO THE USE OF ANY INFORMATION, APPARATUS, METHOD, PROCESS, OR SIMILAR ITEM DISCLOSED IN THIS DOCUMENT, INCLUDING MERCHANTABILITY AND FITNESS FOR A PARTICULAR PURPOSE, OR (II) THAT SUCH USE DOES NOT INFRINGE ON OR INTERFERE WITH PRIVATELY OWNED RIGHTS, INCLUDING ANY PARTY'S INTELLECTUAL PROPERTY, OR (III) THAT THIS DOCUMENT IS SUITABLE TO ANY PARTICULAR USER'S CIRCUMSTANCE; OR

(B) ASSUMES RESPONSIBILITY FOR ANY DAMAGES OR OTHER LIABILITY WHATSOEVER (INCLUDING ANY CONSEQUENTIAL DAMAGES, EVEN IF EPRI OR ANY EPRI REPRESENTATIVE HAS BEEN ADVISED OF THE POSSIBILITY OF SUCH DAMAGES) RESULTING FROM YOUR SELECTION OR USE OF THIS DOCUMENT OR ANY INFORMATION, APPARATUS, METHOD, PROCESS, OR SIMILAR ITEM DISCLOSED IN THIS DOCUMENT.

ORGANIZATION(S) THAT PREPARED THIS DOCUMENT

**Energy and Environmental Strategies (EES)**

**Energy Technologies Enterprises Corporation (EnTEC)**

**Fossil Energy Research Corporation (FERCO)**

**University of California, Irvine**

**Electric Power Research Institute (EPRI)**

**This is an EPRI Technical Update report. A Technical Update report is intended as an informal report of continuing research, a meeting, or a topical study. It is not a final EPRI technical report.**

## NOTE

For further information about EPRI, call the EPRI Customer Assistance Center at 800.313.3774 or e-mail askepri@epri.com.

# CITATIONS

This document was prepared by

Energy and Environmental Strategies (EES)
50 Old Faith Road
Shrewsbury, Massachusetts 01545

Principal Investigator
R. Afonso

Energy Technologies Enterprises Corporation (EnTEC)
P.O. Box 3235
McLean, Virginia 22102

Principal Investigator
S. Tavoulareas

Fossil Energy Research Corporation (FERCO)
23342 S. Point Drive, Suite C
Laguna Hills, California 92653-1470

Principal Investigator
L. Muzio

University of California, Irvine
Department of Mechanical and Aerospace Engineering
4200 Engineering Gateway Bldg.
Irvine, California 92653-3975

Principal Investigators
J. Wei
D. Dunn-Rankin

Electric Power Research Institute (EPRI)
3420 Hillview Ave
Palo Alto, California 94304

Principal Investigators
J. Sanchez
A. Jimenez
J. Stallings

This document describes research sponsored by EPRI. This publication is a corporate document that should be cited in the literature in the following manner:

*Program on Technology Innovation: Research on Ammonium Bisulfate (ABS) Formation in Air Preheaters: Experimental Investigation and Computational Fluid Dynamics (CFD) Modeling.* EPRI, Palo Alto, CA: 2008. 1016164.

# REPORT SUMMARY

Ammonium bisulfate (ABS) formation and deposition is the most common operating problem affecting air preheaters (APHs) in fossil power plants with post combustion $NO_x$ controls that use selective noncatalytic reduction (SNCR) or selective catalytic reduction (SCR). This report describes pilot-scale experiments conducted to better understand ABS chemistry and efforts to develop a computational fluid dynamics (CFD) model of an APH to identify the key phenomena that may affect ABS formation and deposition.

## Background

Earlier EPRI research developed a semiquantitative ABS Fouling Model that provides an indication of whether and where within an air preheater ABS formation and deposition are likely to occur. While this approach has been shown to be qualitatively sound at a number of beta sites, several limitations hinder its predictive capability:

- The prediction of ABS formation temperature is still uncertain.
- The relative contribution of several parameters affecting the location, mechanism, and severity of deposition remains unclear.
- The role of design features specific to particular APHs needs to be elucidated.

EPRI undertook a new project in 2006 to address these uncertainties.

## Objectives

- To improve understanding of ABS formation chemistry
- To identify the key phenomena that may affect ABS formation and deposition in the air heater
- To model ABS behavior using CFD modeling techniques.

## Approach

A multidisciplinary project team conducted experiments to better understand ABS chemistry and also developed CFD models of APHs. In the ABS chemistry experiments, researchers measured ABS formation temperatures using a dew-point meter inserted into an isothermal test section downstream of a pilot-sized natural-gas-burning combustor. In the modeling work, researchers attempted to expand the two-dimensional approach of an existing EPRI APH model into a three-dimensional CFD model of a complete air heater. A single APH flow path was also modeled.

## Results

ABS forms at different temperatures depending on reagent concentration. The experimental measurements made in this study suggest that critical ABS temperatures fall within the range of previous work; but further refinement is still warranted since the two existing previous correlations diverge widely. The results indicate that currently implemented air preheater operating temperatures are conservative with regard to ammonium bisulfate formation.

Researchers used three different methods to develop a three-dimensional simulation of a full-scale APH. Although some results indicated heat transfer and metal temperature predictions, none of the three methods provided satisfactory solutions. A more successful approach was to

model only a single airflow path or basket channel. The primary objective of this simplified approach was to predict fluid and thermodynamic effects inside a single air heater channel while accounting for the air space that exists between the various basket layers of an APH. In order to conduct the single-channel simulation, wall temperatures and inlet boundary conditions were obtained from a case study solved with the Rotational Preheater Metal Temperature (RPHMT) Code. The CFD-predicted flue gas temperatures from this single-channel model were 12.6°F (7 K) higher than those predicted by the RPHMT model. However, these results were based on a different inlet open area and shape than the bulk conditions assumed by the RPHMT model. EPRI will continue to work to obtain additional field data to complete and validate a single-channel model.

## EPRI Perspective

While the ABS formation temperature is better understood as a result of the current effort, there is still lack of understanding of the formation and deposition mechanisms within the air preheater heat transfer surfaces where substantial metal and gas thermal gradients occur. To develop a better understanding of the ABS formation and deposition processes, a bench-scale experiment will be designed, built, and tested. The experiment will simulate a full-scale, single flow channel of an air preheater. The experiment will simulate the temperature-time history in an actual channel from the APH gas inlet (~600°F [589 K]) to the APH gas outlet where the temperature is nominally 300°F (422 K). Gas flow through the device will consist of heated air on one side and simulated flue gas on the other. The simulated flue gas will be heated to about 550°F–600°F (561 K–589 K) and doped with $NH_3$ and $SO_3$ before entering the channel.


## Keywords

Air preheaters
Ammonium bisulfate
$NO_x$ control
Selective noncatalytic reduction
Selective catalytic reduction
Computational fluid dynamics

# ABSTRACT

Fouling of air preheaters as a result of ammonium bisulfate (ABS) formation is a common problem in installations with selective noncatalytic reduction (SNCR) or selective catalytic reduction (SCR) post-combustion $NO_x$ controls. EPRI previously developed a useful ABS Fouling Model but several limitations hinder the predictive capability of the existing model. This project addressed these limitations by undertaking laboratory experiments to improve prediction of ABS formation temperatures and by attempting to develop a computational fluid dynamics (CFD) model of an air preheater. The lab work indicates that currently implemented air preheater operating temperatures are conservative with regard to ammonium bisulfate formation. In the CFD modeling part of the project, regenerative APH full-scale three-dimensional simulation was attempted using three different methods. Although some results indicated heat transfer and metal temperature predictions, none of the three methods provided satisfactory solutions. Flue gas flow through a single channel was also simulated using the FLUENT code with an overall objective of predicting thermodynamics and fluid dynamics effects inside the channel and between layers. Preliminary CFD results predicted temperatures of 312°F (429 K) at the cold layer outlet compared to 300°F (422 K) predicted by the Rotational Preheater Metal Temperature (RPHMT) model. Further modeling and laboratory work is planned to improve understanding of ABS formation and deposition and to develop a better predictive air preheater model.

# LIST OF ACRONYMS

| | |
|---|---|
| APH | air preheater |
| ABS | ammonium bisulfate |
| CFD | computational fluid dynamics |
| EES | Energy and Environmental Strategies |
| EnTEC | Energy Technologies Enterprises Corporation |
| EPRI | Electric Power Research Institute |
| FERCO | Fossil Energy Research Corporation |
| RHMT | Rotational Preheater Metal Temperature |
| SNCR | selective noncatalytic reduction |
| SCFM | standard cubic feet per minute |
| SCR | selective catalytic reduction |
| UCI | University of California, Irvine |
| UDF | user-defined function |
| UDS | user-defined scalar |
| VOF | volume of fluid |

# CONVERSIONS USED IN THIS REPORT

°C = (°F-32) x 5/9

°C = K – 273.15

°F = (°C x 9/5) +32

°F = (1.8 x K) – 459.67

K = (°F +459.67)/1.8

K = (°C) + 273.15

1°F = 0.5556°C (temperature increment)

1°F = 0.5556 K (temperature increment)

1 ft = 30.48 cm

1 in. = 25.4 mm

1 mm = 0.0393 in.

1 in. = 0.0254 m

1 $in.^2$ = 0.000645 $m^2$

1 scfm = 472 $cm^3$s

1 $cm^3$ = 0.061 $in.^3$

1 lb/hr = 0.000126 kg/s

1 $kg/m^3$ = 0.062 $lb/ft^3$

J/Kg-K= 1 J/Kg-°C = 2.39 E-4 Btu/lb-°F

W/m- K = 0.578 Btu/hr-ft-°F

$W/m^3$ = 0.0966 $Btu/hr-ft^3$

# CONTENTS

# 1
# BACKGROUND AND OBJECTIVES

## Background

Utility installations of post-combustion $NO_x$ controls (selective noncatalytic reduction [SNCR] and selective catalytic reduction [SCR]) have experienced varying degrees of operating problems with the air preheaters (APHs). Fouling of air preheaters as a result of ammonium bisulfate (ABS) formation and deposition is the most common phenomenon.

Beginning in 1997–98, Energy Technologies Enterprises Corp. (EnTEC), under contract with the Electric Power Research Institute (EPRI), carried out a utility survey to document operating problems experienced by units retrofitted with SNCR and SCR systems, collected relevant data, and summarized the results in a report, along with recommendations on future research. EnTEC developed a beta version of the *Air Preheater Fouling Guidelines*, a software model based on a previously EPRI-developed, Excel-driven spreadsheet to predict rotating metal temperatures of regenerative APHs called the Rotational Preheater Metal Temperature (RPHMT) model. A guidance document and a cost-benefit model to evaluate alternatives for air heater fouling mitigation were also included in the guidelines, which were released officially in 2004 [2].

The predictive APH ABS Fouling Model developed during this effort has been well-documented (see References 1, 2, 4, and 5), and its application at various beta sites has indicated a good level of predictability and applicability. In other words, the model performs quite well within the framework for which it was intended. This framework provides a platform that essentially identifies a region of ABS formation/deposition within the APH, which is then integrated with semiquantitative analyses of the potential severity for ABS fouling. A typical graphical output of the existing model, indicating the region of the APH where potential ABS can form and deposit, is shown in Figure 1-1.

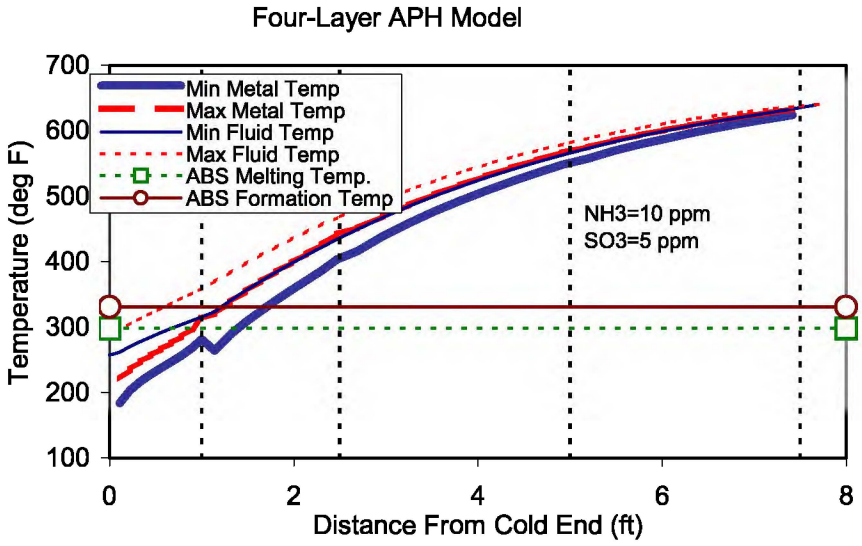


**Figure 1-1**
**Sample APH Model Results**

The existing approach integrates this information with other known design/operating considerations for a particular APH to assign a fouling severity potential or index as summarized below from the 2004 Guidelines report:

> …the ABS Fouling Model provides an indication of whether and where within the APH ABS formation and deposition are likely to occur. It does not define an amount or rate of ABS deposition in the APH. The amount and rate of ABS deposition in the APH heating element surfaces are impacted by, among others, the following physical/design factors
>
> - Type of heating element plate (e.g. closed vs. open, pitch)
> - Location of ABS formation zone relative to element layer split
> - Distance of ABS formation zone from the cold-end
> - Condition and material of heating element surface
> - Location and performance of soot blowers
> - High- vs. Low-dust configuration
>
> It is evident from this, that multiple considerations must go into determining the Fouling Severity levels, based on the graphical results of the ABS Fouling Model as well as the parameters above.
>
> The following ranking for each of the parameters above is proposed to be used in determining Fouling Severity. Users must select the options applicable to their cases and add the corresponding scores to develop a total.
>
> **Heating element**
>
> - Closed - (1)
> - Open - (3)

**Location of ABS formation zone relative to element layer split**

- Across split - (3)
- *Within single layer - (1)*

**Distance of ABS formation zone from the cold-end**

- *Deep - > 24 in - (3)*
- *Moderate - 18-24 in (2)*
- *Short - < 18 in (1)*

**Condition and material of heating element surface**

- *Carbon steel - (3)*
- *LACR - (2)*
- *Enamel - (1)*

**Location and performance of sootblowers**

- *Hot-end (conventional) (3)*
- *Cold-end (conventional)- (1)*
- *High-energy - (0)*

**High- vs. Low-dust configuration**

- *High-dust - (1)*
- *Low-dust - (3)*

Note that two of the factors above - "location of ABS formation zone relative to element layer split" and "distance of ABS formation zone from the cold-end" - are determined by examining the graphical results of the ABS Fouling Model, while the other four are all physical and design characteristics of the APH.

These factors can be combined to provide guidance in determining the Fouling Severity input to the model as follows:

- 6-9: negligible - no ABS induced outages
- 10-14: medium - 1 to 3 outages per year
- 15-18: severe - 4 to 6 outages per year …"

Although this approach has been shown to be qualitatively sound as "validated" by a number of beta sites [1], it is also recognized that several limitations hinder the predictive capability of the existing model:

- The prediction of ABS formation temperature is still uncertain. Two prevailing correlations (Hitachi and Radian) result in significantly different ABS formation temperatures for similar operating conditions. Further insight into this will help pinpoint the temperature regime of ABS formation.

- Once ABS is formed, the key issue is if/where/how it deposits on the APH plates. Much has been learned during the EPRI project, but much is still unknown, including the roles and relative contribution of several parameters:
  - Deposition mechanisms - ABS aerosol versus gas diffusion
  - ABS viscosity (stickiness)
  - APH plate surface conditions (for example, smooth versus rough or corroded)
  - Aerodynamic impact of special flow regimes (for example, layer splits)
  - Role of fly ash contribution to overall deposit (for example, deposit growth versus erosive action)
- It is expected that these (and perhaps others) play a role in the initial deposition and rate of accumulation of ABS, but no formal modeling or analyses have been performed to date.
- Unique design features (for example, configuration, type of plates, inlet flow/temperature profiles) of each air heater may play important roles as well.

## Objectives

As a result of the above uncertainties, EPRI decided to undertake a new project in 2006 aimed at closing the gaps identified. The objectives of this project were to:

- Enhance the industry's understanding regarding the formation chemistry of ABS
- Identify the key phenomena that may affect ABS formation and deposition in the air heater
- Attempt to model ABS behavior using computational fluid dynamics (CFD) modeling techniques

# 2
# TECHNICAL APPROACH

To accomplish the stated objectives, EPRI assembled a complementary (multi-disciplinary) technical team made up of the following:

- EnTEC/Energy and Environmental Strategies (EES) –APH fouling expertise and overall project management
- Fossil Energy Research Corporation (FERCO)/University of California, Irvine (UCI)– ABS chemistry and lab/pilot-scale testing
- EPRI – CFD modeling development

Full descriptions and results of these efforts are documented in two reports (included here as Appendices A and B). Consequently, only brief summaries are provided in this section.

### Experiments to Develop a Better Understanding of ABS Chemistry - (FERCO/UCI)

The experimental setup to measure the formation temperature of ABS required an environment simulating that of the flue gas in a coal-firedpower plant, including temperatures and chemical composition controls. In this case, a pilot-sized natural-gas-burning combustor was used to create temperatures above 700°F (644 K). Simulation of the flue gas composition was accomplished by directly injecting $NH_3$ gas, $SO_2$ gas, and diluted $H_2SO_4$ solution into the combustor. Concentrations of $NH_3$ and $H_2SO_4$ in the flue gas were controlled by input versus output calibration relationship, along with both $SO_3$ and $NH_3$ measurements.

To measure ABS formation temperatures, a dew-point meter (a Conserver IV Acid Dew-Point Monitor manufactured by Land Instruments) was inserted into an isothermal test section downstream of the combustor. This instrument is designed to measure sulfuric acid dew points in flue gas and is used in power plants to prevent cold-end corrosion of system components. To adapt its traditional use to the current task, an approach was followed using that developed by Breen Environmental Solutions for their ABS fouling probe, which is also based on the Land dew-point meter. Figure 2-1 below shows a schematic of the probe.

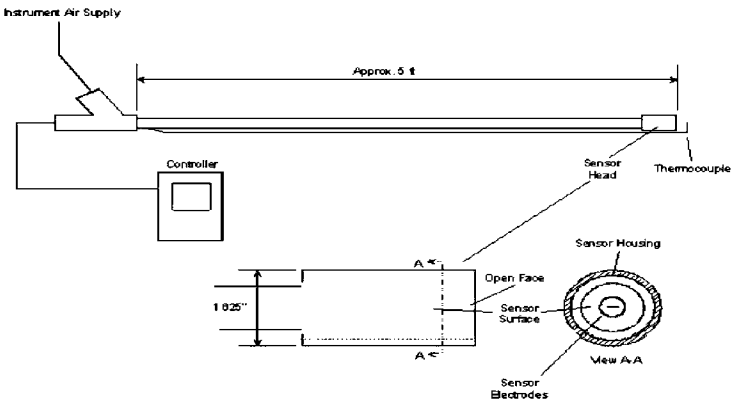


**Figure 2-1**
**Schematic of Land Dew-Point Meter**

## CFD Modeling (EPRI)

As stated in Section 1, the existing ABS fouling guidelines are based on EPRI's Rotational Preheater Metal Temperature (RPHMT) model. This code is a two-dimensional numerical model that predicts temperatures in the axial (gas flow direction) and peripheral direction at a specified radial distance. The RPHMT model provides the ability to quickly predict heat transfer effects due to changes in operating parameters, such as gas side temperatures or rotational speed. Other applications include the effects on metal temperature distribution due to design changes, such as the removal of metal elements or the change of element material or design geometry. The code has been widely validated at many beta sites.

In the present effort, it was desired to expand the two-dimensional approach of the existing EPRI APH model into a three-dimensional CFD model of a complete air heater. The objective of this model is to predict fluid and metal temperatures and to account for the impact of the rotational baskets within the intermediate spaces between basket layers. The three-dimensional APH was to be coupled with another CFD-based model of a "single channel" or a limited number of heat transfer plate channels to include species mixing and thermal effects. This was done in order to map locations within the APH baskets where ABS may form under a given set of conditions and investigate design adjustments to optimize heat transfer and reduce the opportunity for ABS formation and/or deposition.

### *Full-Scale APH Model*

The three-dimensional model incorporated the domain of both air and gas sides; thus, the model was developed to provide air side as well as gas side temperatures. The metal matrix of the air heater was simulated using a number of approaches, but none included the actual geometry of the metal baskets. During this effort, dimensions and variables similar to an existing three-layer EPRI APH model case were used for model development. The model required a user-defined subroutine to calculate the convective heat-transfer coefficient "h" and to simulate the heat transfer between the gas phase and the metal baskets. ANSYS/Fluent was the contractor that developed the subroutine.

### *Single-Channel Model*

A single APH flow path was also modeled. The geometry included three channels to represent the hot, intermediate, and cold layers. The sections between layers were modeled using planes of symmetry in order to simulate an isotropic condition. This functionality creates a mirror plane at the selected surface and assumes identical conditions on both sides of the face. This approach assumes that fluid coming out of one layer goes right into the next layer. The sections between layers were modeled using the standard k-e turbulence model, and the channel sections were modeled as laminar flow zones.

# 3
# RESULTS

Full results and discussion are included in the two reports included here as Appendices A and B. The key findings and discussion are summarized in this section.

## FERCO/UCI – ABS Experiments

Figure 3-1 presents the main findings from the experimental work.

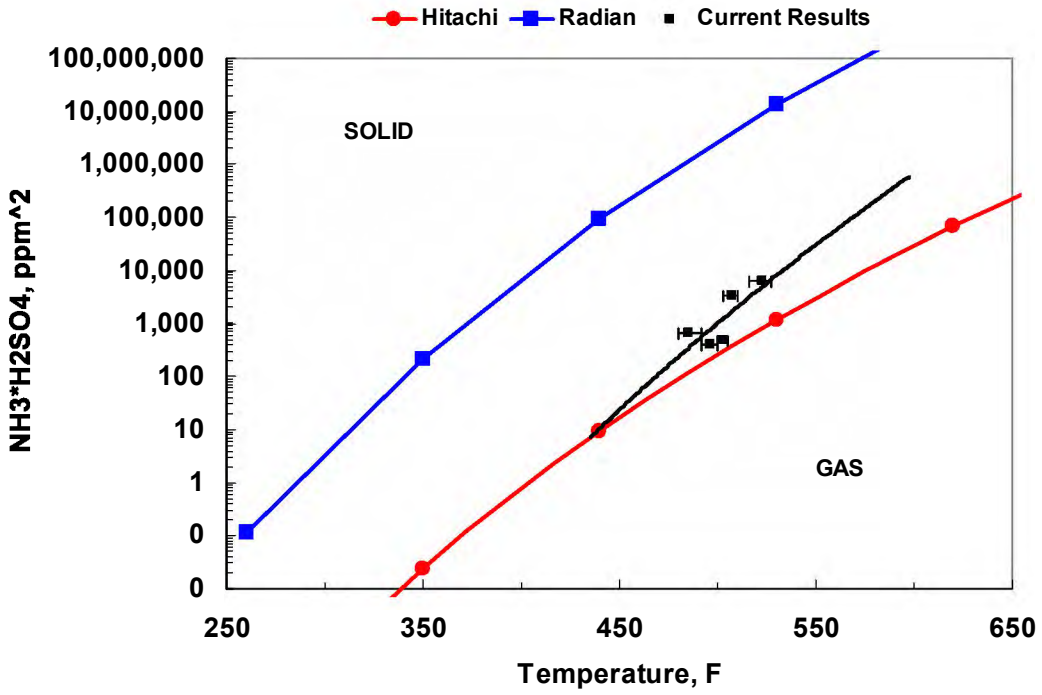


**Figure 3-1**
**Reactant Concentration vs. ABS Formation Temperature**

These results fall between the Radian and Matsuda curves, tending more toward the Matsuda curve than the Radian curve. It is believed that the resulting curve occurs at a lower temperature than that of Matsuda, possibly as a result of the experimental procedure used in that study. However, there are several other factors that warrant consideration in the current study.

One reason for the noticeable difference is that Radian results assume ideal clean gas conditions with no condensation nuclei to assist the process. Although the FERCO facility is a natural-gas-burning combustor, the combustor has been used for various other research projects. Several of these include the injection of fly ash and catalyst powder. Impurities present in our combustor inputs or any of residuals mentioned may serve as nuclei for heterogeneous nucleation, causing the ABS to condense sooner than it would otherwise and, thus, effectively raising the ABS formation temperature detected.

Secondly, there is a boundary layer between the gas approaching the sensor and the surface of the sensor. Condensation could start to occur in the boundary layer at a higher temperature than the sensor temperature. In this case, the higher temperature noted in the current procedure may be a better indication of the ABS dew point. This requires more study. Further, it is important to recognize that the dew-point probe approach simulates only ABS formation due to gas-phase diffusion and condensation onto a cold surface, as in an APH heat transfer plate, but it does not simulate the rapid gas cooling that occurs within the APH that is conducive to ABS aerosol formation.

At present, the existing EPRI ABS Fouling Model uses the Radian temperature curves; however, manufacturers often provide guidance using a higher temperature of formation as do SCR catalyst vendors.

## EPRI – CFD Modeling

The regenerative APH full-scale three-dimensional simulation was attempted using three different methods. Although some results indicated heat transfer and metal temperature predictions, none of the three methods provided satisfactory solutions. The algorithms derived from the RPHMT code, which are based on global heat transfer correlations of the air heater, did not yield satisfactory results with the volumetric cell approach used by the FLUENT code. Further development between ANSYS/Fluent and EPRI is necessary to test solutions for a more robust model.

Flue gas through a single channel was also simulated using FLUENT. The overall objective was to predict thermodynamics and fluid dynamics effects inside the channel and between layers. When the model is fully developed, results should support the project team's further investigation of the phenomena that may impact ABS formation and deposition inside APHs.

Channel dimensions and boundary conditions were obtained from the RPHMT model. Preliminary CFD results predicted temperatures of 312°F (429 K) at the cold layer outlet compared to 300°F (422 K) for the RPHMT model (minimum temperatures). This approach shows good potential to focus on the development of the "single" channel model by developing its capabilities in the chemical/fluid dynamics area and integrating it directly with temperature profiles from the RPHMT model.

## EnTEC/EES

EnTEC/EES reviewed several formation and deposition phenomena of ABS as input to the CFD model being developed by EPRI. This included several documents identified during a literature search on ABS formation research to support and supplement the previous work done in this area. This effort confirmed that this research area has not been active recently and—more importantly—that the previous efforts undertaken by EnTEC (1998–2002) and FERCO (2003) have captured the available database adequately. It is appropriate to note that these separate efforts yielded similar conclusions and provided further justification for the current experimental work in progress.

Although papers have addressed ABS-related deposition and impacts, no new fundamental ABS formation research has been identified. The exception is in the area of atmospheric

ammonium/ABS transformations. A number of such papers were reviewed, but they provided no relevance to the current project.

EnTEC also began to investigate other areas identified as main contributors to the ABS deposition phenomena:

- Deposition mechanisms - ABS aerosol versus gas diffusion

  This is important because gas or metal temperatures drive the deposition. It is hoped that this can be addressed through additional experimental work (possibly a second phase to FERCO's experiments). Nothing has been found in the literature beyond the references to the split between aerosol/gas diffusion in Radian's report. A third mechanism is likely the condensation on fly ash particles. Some work is being done by EPRI and others in the area of $SO_3$ uptake by fly ash that may be of interest and have relevance to this project.

- ABS viscosity (stickiness)

  This will be important as it relates to the adhesion forces that influence deposition as well as erosive forces. The literature search to date has been without much success in this area. Quantitative data may be possible only through experimental work. However, FLUENT can model adhesion forces.

- APH plate surface conditions (for example, smooth versus rough or corroded)

  This is possibly the "easiest" to model. FLUENT should be able to accept surface roughness conditions and appropriately reflect these in the developed boundary layer.

- Aerodynamic impact of special flow regimes (for example, layer splits)

  This will be appropriately modeled within FLUENT simply through the geometric modeling of the layer split areas. EnTEC has provided initial inputs on this and will refine them further as the modeling effort is further developed.

- Role of fly ash contribution to overall deposit (for example, deposit growth versus erosive action)

  This is related to "competition" between ash accumulating and ash being an erosive force that actually "cleans" the initial deposits. It is related to the viscosity/stickiness issue above. This still needs to be addressed in the future.

In addition, EnTEC/EPRI investigated and determined the following regarding how to model several key parameters:

- ABS viscosity: This can be modeled within FLUENT.
- Surface smoothness/roughness: FLUENT handles this adequately. There are several different approaches that can be followed; most likely, FLUENT will model the boundary layer at the plate.
- Aerodynamic impact of special flow regimes (for example, layer splits): This can be modeled by FLUENT through the geometric modeling of the layer split areas.
- Role of fly ash contribution to overall deposit (for example, deposit growth versus erosive action): More discussion and research may be needed on this. It is difficult to model particles and/or droplets to collide/merge before they reach the surface (plate of the air heater). FLUENT would handle this through particle "saltation" and "rebound" factors.

## Summary

The project has been a valuable effort toward the understanding and development of ABS behavior in APHs. Given the extensive previous work conducted by EPRI in this area and considerable expertise gained, the current work has focused on elevating the overall ability to model and predict ABS formation/deposition in the APH. Specifically, this effort addresses two main areas: 1) refinement of ABS formation temperatures, driven by the lack of agreement by previous researchers; and 2) development of a modeling capability to include not only the APH thermal performance (already adequately done by the RHPMT), but primarily the multiple parameters that affect the formation and deposition of ABS within the APH heat transfer surfaces.

In both areas, progress has been made, but much remains to be learned. The experimental setup suggested ABS temperatures that were within the range of previous work, but given that wide range, further refinement is still warranted. With respect to the modeling effort, it was determined that a large, full APH CFD model is neither simple nor warranted—given the existence of the RPHMT model to calculate thermal performance. However, further development of a "single" channel model where reaction kinetics and aerodynamic behavior can be incorporated seems an achievable and worthwhile objective.

## Future Work

Given the results obtained and issues identified during this project, further investigation is warranted, specifically in the area of ABS formation. To that extent, the following summarizes a proposed scope of work, the results of which will be integrated into the existing effort.

Although the ABS formation temperature is better understood as a result of the current effort, there is still lack of understanding of the formation and deposition mechanisms within the APH heat transfer surfaces, where substantial metal and gas thermal gradients occur. To repeat some of the main outstanding issues:

- Does the ABS form primarily as an aerosol in the entrained gas as it diffuses toward the cooler metal surface, then deposit?
- Does the ABS form primarily on the metal surface of the baskets?
- What role does the gap between the baskets play in the ABS deposition process?
- What role does ash play in the formation and deposition process? Is it an important source of surface area for ABS nucleation?

An understanding of these processes is needed in order to develop a better predictive APH model. Such a model can, in turn, be used to develop approaches to minimize ABS/ash deposition.

### *Proposed Approach*

To develop a better understanding of the ABS formation and deposition processes, a bench-scale experiment will be designed, built, and tested. The experiment will simulate a full-scale, single-flow channel of an APH. The experiment will simulate the temperature-time history in an actual channel from the APH gas inlet (~600°F [589 K]) to the APH gas outlet where the temperature is nominally 300°F (422 K). Gas flow through the device will consist of heated air on one side and

simulated flue gas on the other. The simulated flue gas will be heated to about 550°F–600°F (561 K–589 K) and doped with $NH_3$ and $SO_3$ before entering the channel. Figure 3-2 shows a conceptual sketch of the device.

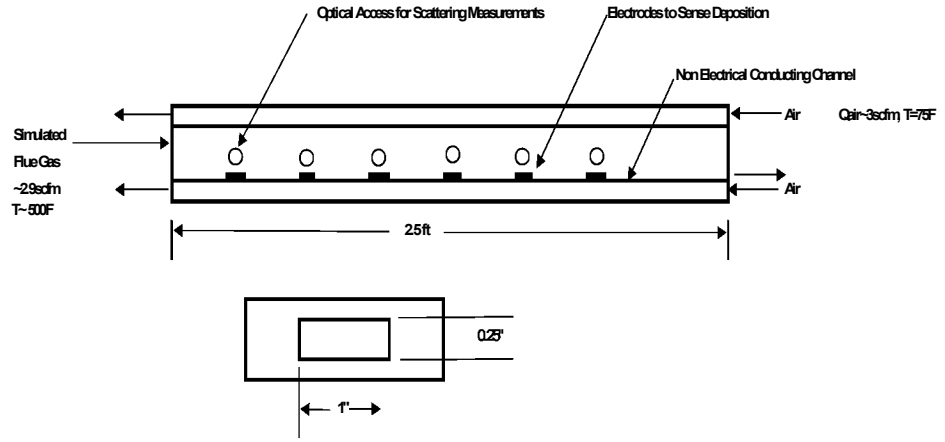


**Figure 3-2**
**Conceptual Sketch: Single-Channel Experiment**

The detailed experiment will be designed as part of this project, and the concept involves the following features:

- Optical access along the length of the channel. Optical forward scattering measurements will be made to determine the formation of an ABS aerosol in the entrained phase.
- The channel will be fabricated from an electrically insulating material. Electrodes will be incorporated onto the surface. These electrodes will be used to detect the formation and/or deposition of ABS on the surface following the approach of existing acid dew-point sensors.
- Temperature sensors will be incorporated to measure both the gas and wall temperatures along the length of the channel.

The flow will be set up to simulate full-scale flow through a single channel. The primary variables to be investigated include temperature and $NH_3$ and $SO_3$ concentrations.

The proposed task breakdown is shown below:

Task 1: CFD experimental design

Task 2: Hardware design and fabrication

Task 3: System checkout

Task 4: Testing

Task 5: Analysis and reporting

# 4
# REFERENCES


1. R. Afonso, C. Biggs, J. Billings, J. Urbas, S. Tavoulareas, J. Stallings, "Air Preheater Fouling Assessments: Application and Results of EPRI's APH Model at Several Power Plants," EPRI/DOE/EPA Mega Symposium, Washington, DC (2004).
2. *Air Preheater Fouling Guidelines, Version 1.0.* EPRI, Palo Alto, CA: 2004. 1004142.
3. L. Muzio, Q. Qader, J. Schardin, "A Review of ABS Formation Temperature Data" FERCO report (prepared for EPRI), 2003.
4. L. Marshal, R. Afonso, S. Tavoulareas, J. Stallings, "Air Preheater Fouling due to Ammonium Bisulfate: Application of EPRI's Model at OPG's Nanticoke and Lambton Stations," EPRI/DOE/EPA Mega Symposium, Washington, DC (2003).
5. R. Afonso, L. Marshal, S. Tavoulareas, J. Stallings, "Prediction and Mitigation of Air Preheater Fouling due to Ammonium Bisulfate," EPRI/DOE/EPA Mega Symposium, Chicago, IL (2001).
6. *Assessment of APH Fouling Due to Utilization of SNCR and SCR Systems.* EPRI, Palo Alto, CA: 1998. GC-111797.
7. J. M. Burke and K. L. Johnson, "Ammonium Sulfate and Bisulfate Formation in Air Preheaters," EPA, 1982, 600/7-82-025a.

# A
# ABS PILOT-SCALE EXPERIMENTS (FERCO/UCI)

**Paper #H12** **Topic: Stationary**

5th US Combustion Meeting
Organized by the Western States Section of the Combustion Institute
and Hosted by the University of California at San Diego
March 25-28, 2007

## Formation Temperature of Ammonium Bisulfate at Simulated Air Preheater Conditions

*J. Y. Wei[1], L. J. Muzio[2] and D. Dunn-Rankin[1]*

[1]*Department of Mechanical and Aerospace Engineering, University of California, Irvine, CA, 92697-3975*

[2]*Fossil Energy Research Corporation, Laguna Hills, CA, 92653*

Ammonium bisulfate (ABS) can form in the air preheater of coal-fired power plants when the ammonia injected for selective catalytic reduction or selective non-catalytic reduction of $NO_x$ reacts with $SO_3$ formed from the sulfur in the coal. Ammonium bisulfate is a sticky condensate, and accurate determination of its formation temperature can help prevent preheater pluggage and lower the frequency of cleaning. In this work, the condensation temperatures of ABS are measured in simulated flue gas containing various combinations of reactant concentrations ([$NH_3$] and [$SO_3$]). Flue gas with composition similar to that of a power plant is produced by a pilot-scale combustor, and the formation temperature is measured with an acid dew-point meter. Although the instrument was designed for acid dew-point monitoring, a modified methodology and data analysis were developed to determine ABS formation. The measured ABS dew-point temperatures are compared to several existing experimentally obtained and thermodynamically determined curves in the range of product of reactant concentration 100 ~ 2500 $ppm^2$. The results indicate that currently implemented air preheater operating temperatures are conservative with regard to ABS formation.

## 1 Introduction

In a coal-burning power plant, selective catalytic reduction (SCR) and selective noncatalytic reduction (SNCR) processes are often used to reduce the $NO_x$ emissions downstream of the furnace. However, $NH_3$ exiting the process, in combination with the $SO_3$ present in the flue gas, may at sufficiently low temperature react and result in the undesirable formation of ammonium bisulfate (ABS). ABS formation creates problems at various locations in a power plant. ABS may clog the $NH_3$ injection nozzles in the SCR, affecting the $NH_3/NO_x$ ratio and leading to insufficient $NO_x$ reduction. At low temperatures, ABS can form on the catalyst, reducing the overall activity of the catalyst. A key balance-of-plant impact is the deposition of ABS on the surface of the air preheater, plugging the gas passages and causing surface corrosion. These consequences impair the operation and affect the reliability of the $NO_x$ reduction process and the air preheater. Furthermore, costly unit outages may be required to wash the air preheater [1]. Although the results of tests conducted in Japan showed no evidence in decline in air preheater thermal efficiency with ABS deposition, the issues of plugging, corrosion, and long-term operational life remain [2].

Therefore, for better system design, with improved operation and maintenance performance, it is important to identify the mechanisms and parameters affecting the formation of ABS. We investigate the formation (or condensation) temperature of ABS because these values dictate how much $NH_3$ slip an air preheater can tolerate.

Several studies have explored the formation temperature of ABS, although little had been done experimentally. Most existing studies on ABS involve calculations of ABS equilibrium constants using thermodynamic analysis. For example, Kelley [3] et al. used calorimetric determinations to evaluate specific heats of ABS, while Scott and Cattell [4] measured the partial pressure ratio of $NH_3$ over ABS in the temperature range of 45–180°C in the dry system of $H_2SO_4$ and $NH_3$. Later, in combination with the thermodynamic analysis, Radian utilized results from various cooperating power plants and developed a kinetic model to predict the formation and deposition of ammonium sulfates, including ABS. Radian identified the following principal chemical reactions for the formation of ABS:

$$NH_3 + SO_3 + H_2O \rightleftharpoons NH_4HSO_4 \quad (1)$$

$$NH_3 + H_2SO_4 \rightleftharpoons NH_4HSO_4 \quad (2)$$

$$SO_3 + H_2O \rightleftharpoons H_2SO_4 \quad (3)$$

Radian especially noted the importance of including the often-ignored chemical reaction (3) in the chemical equilibrium calculations. The presence of $H_2SO_4$ reduces the amount of $SO_3$ available in the flue gas to react with $NH_3$ and tends to reduce ABS formation temperature [1].

On the other hand, Matsuda et al. [2] took an experimental approach and defined the vapor pressure of ABS as the product of vapor pressures of $H_2SO_4$ and $NH_3$ based on reaction (2). Matsuda passed a gas mixture containing the two reactants through a 17-mm ID, 900-mm long glass tube in an electric furnace. Twelve quartz tubes were placed inside the tube along its length, and the furnace was set up with an axial temperature gradient from 360°C to 100°C. ABS deposit was recovered from each plate, and the temperature of the section with the majority of the deposit was taken to be the formation temperature at those reactant concentrations. The resulting ABS formation curves from Radian and Matsuda et al. are plotted together in Figure A-1.

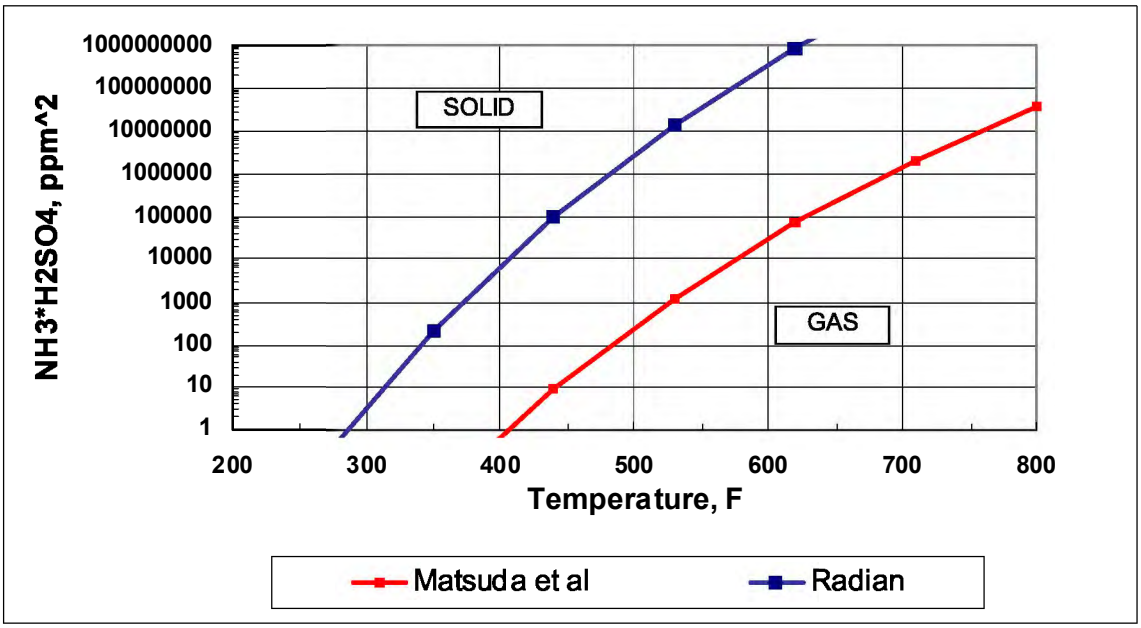


**Figure A-1**
**Radian and Matsuda et al. ABS Formation Temperature Curves**

In Figure A-1, the difference between the two formation temperatures at each reactant combination is above 120°F. The source for the much higher ABS formation temperature that Matsuda et al. report may be the non-isothermal nature of their experimental setup. In the electric furnace, with the intentional axial temperature gradient, a radial temperature gradient is unavoidable also. It is, therefore, hard to identify where the ABS starts to form because of the temperature difference between the bulk gas and the wall.

In addition, although an ABS deposit does not lower the thermal efficiency of the air preheater [7] directly, operating the air preheater according to an accurate, lower ABS temperature curve would increase the air preheater thermal efficiency substantially since more heat can be recycled back to the power generation system. The discrepancies between the two ABS formation curves in Figure A-1 and the potential increase in air preheater thermal efficiency motivate our experiments to determine an accurate ABS formation curve under a simulated flue gas environment.

# 2 Experimental Setup

## 2.1 Approach

To measure the formation temperature of ABS, we must first create an environment simulating that of the flue gas in a coal-fired power plant. This includes temperatures and chemical composition controls. We use a pilot-sized natural-gas-burning combustor to create temperatures above 700°F. Simulation of the flue gas composition is accomplished by directly injecting $NH_3$ gas, $SO_2$ gas, and diluted $H_2SO_4$ solution into the combustor. We can control the concentration of $NH_3$ and $H_2SO_4$ in the flue gas according to the reactant concentration input versus output calibration relationship. The actual measurement of ABS formation temperature is conducted using a dew-point meter inserted into an isothermal test section downstream of the combustor.

## 2.2 Apparatus

### 2.2.1 Combustor

The combustor used to create high-temperature flue gas is approximately 12 feet tall and 1½ feet in diameter. The combustion chamber on the top part of the combustor is 3 feet tall and 1½ feet in diameter, and it is followed by a Venturi section with a throat diameter of 3 inches. This is then followed by a plug flow section that is 9 feet tall and 6 inches in diameter surrounded by refractory. Flue gas flow exits from one opening at the bottom of the combustor; another opening adjacent to it allows additional air to flow in for temperature control. The combustor has sampling ports along the sides for injection and sampling purposes. The main combustor inputs—air and natural gas—are metered by rotometers, and the ratio can be adjusted to the desired combustion condition. Also, thermocouples are located at various positions to monitor the temperature change in the combustor along the axial direction [5].

Immediately downstream of the combustor, we constructed a 5 foot long, 6 inch diameter straight section of stainless steel with a tee on one end. This part of the ducting is wrapped with 1 inch of KaoWool for thermal insulation. The creation of this temperature- and velocity-uniform region is an important element of the experiment, and it facilitates the insertion of the dew-point probe.

### 2.2.2 Flue Gas Composition

For the formation of ABS, sufficient concentrations of the reactants $NH_3$, $SO_3$, and $H_2O$ are required. Both $NH_3$ gas and $H_2SO_4$ solution (the decomposition of the latter produces $SO_3$ and $H_2O$) are injected using water-cooled probes through the ports on the side of the combustor. Whereas $NH_3$ is supplied from a high-purity gas tank and mixed with the carrier air in the probe before injection, a diluted $H_2SO_4$ solution (0.6 M) is sprayed into the combustor using a peristaltic pump and a twin-fluid atomizer with carrier air. To enhance mixing, both probes are oriented to accomplish counterflow injections because prior studies in this facility indicate that injected material is uniformly mixed across the combustor.

During preliminary experiments, we found that injecting additional $SO_2$ was necessary to obtain our desired $SO_3$ concentration because, at high combustor temperatures (above 700°F), chemical equilibrium codes show that the decomposition of $SO_3$ into $SO_2$ is highly preferred [6]. The $SO_2$ encourages the decomposition of $SO_3$, and the $SO_2$ is directly mixed into the main air supply of the combustor.

Both $O_2$ and $SO_2$ concentrations in the flue gas are monitored using continuous gas analyzers. This ensures a consistent combustor operation and flue gas composition. The nominal combustor operating condition is described in Table A-1.

**Table A-1**
**Nominal Combustor Operating Condition**

| Combustor input | Unit | Condition |
|---|---|---|
| Main air | scfm | 16.2 |
| Natural gas | scfm | 1.07 |
| $SO_2$ | scfm (ppm) | 0.0427(2000) |
| $H_2SO_4$ solution, 0.06 N | cc/min (ppm) | 25.6(30) |
| $H_2SO_4$ carrier air | scfm | 0.25 |
| $NH_3$ gas | scfm (ppm) | 6.4x10−4~3.2x10−3(30 ~ 150) |
| $NH_3$ carrier air | scfm | 0.63 |
| $O_2$ | % dry | 8 |
| $H_2O$, combustion | % | 12 |
| $H_2O$, $H_2SO_4$ injection | % | 14.7 |
| Total flow | scfm | 21.33 |

### *2.2.3 Reactant Concentration*

Being able to quantitatively control the amount of reactant present in the combustor is crucial to obtaining accurate condensation temperature measurements. Therefore, reactant concentrations present in the simulated flue gas, [$NH_3$] and [$SO_3$], are verified by chemical sampling and analysis. $NH_3$ concentration is determined by sampling a measured portion of the flue gas and then collecting the $NH_3$ in a series of impingers filled with a weak (0.02 M) sulfuric acid solution. An ionic-strength-adjusting solution is then added to the sample, and gas phase $NH_3$ can be measured by an $NH_3$ ion-specific electrode. The controller of the electrode displays an output corresponding to the $NH_3$ concentrations.

$SO_3$ concentration is determined also by sampling a measured portion of the flue gas using the controlled condensation method and titrating the sample for the sulfate ion. The controlled condensation method involves passing the flue gas through cooling coils and a frit. Circulated, heated water maintains the temperature of the flue gas sampled between the $H_2SO_4$ and $H_2O$ dew points. Thus, $H_2SO_4$ in the flue gas condenses, while $H_2O$ remains in the gas phase. The condensed $H_2SO_4$ is then collected by rinsing the coils and frit with distilled water. The content of $SO_3$ can be determined through titration with $BaCl_2$ for sulfate ion using a Thorin indicator. $SO_3$ concentration can then be calculated from the titration results and the metered flue gas volume [7].

### *2.2.4 Land Dew-Point Meter*

Breen Environmental Solutions is developing an ABS fouling probe based on the Land dew-point meter. The device is being developed to measure a fouling index, not necessarily the ABS formation temperature, to help prevent the formation of ABS. The current study adopted the same basic approach to determine ABS formation temperature [8].

The dew-point meter used to detect the ABS formation temperature is the Conserver IV Acid Dew-Point Monitor manufactured by Land Instruments. The instrument is designed to measure sulfuric acid dew points in flue gas for the purpose of increasing plant efficiency and preventing corrosion of system equipment. It consists of a 5 foot long probe with a sensor tip for condensation detection on one end. The sensor tip has a glass surface with a ring and an inner electrode in the center. Compressed air is drawn from the other end of the probe and pumps through the inner part of the probe to cool the sensor tip. A diagram of the probe is shown in Figure A-2.

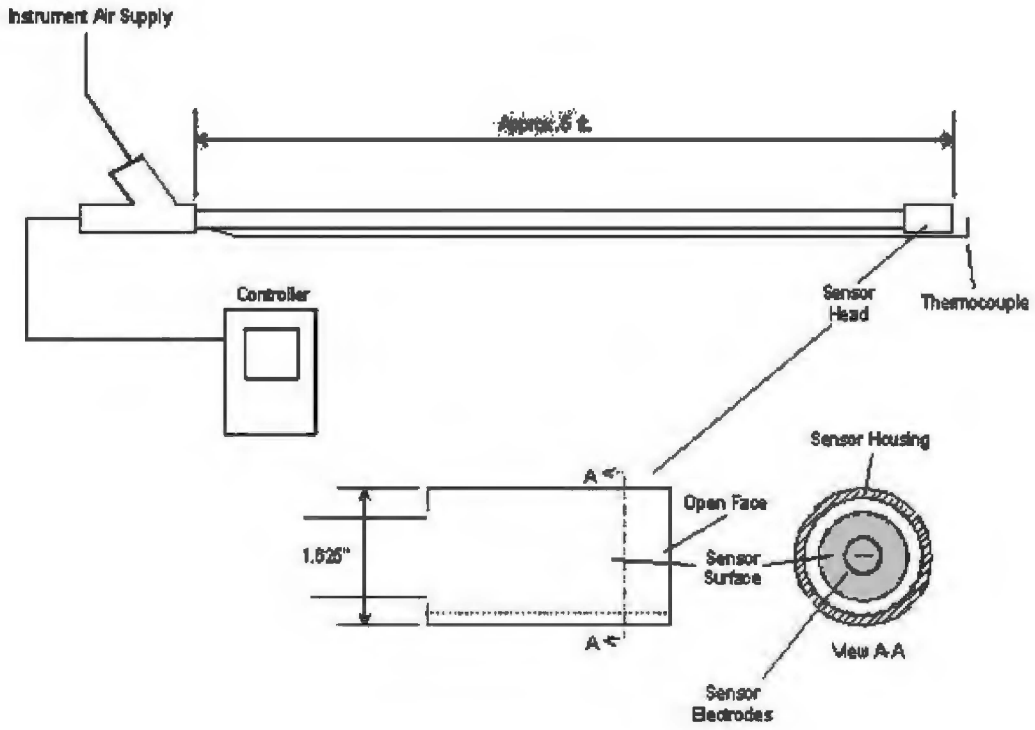


**Figure A-2**
**Schematic of Land Dew-Point Meter**

There are two built-in thermocouples on the dew-point meter, one by the sensor tip for the flue gas temperature, and the other underneath the sensor tip to measure the glass tip temperature. When the dew-point temperature of a substance is reached, condensate starts to form. The condensate on the glass surface completes the circuit between the two electrodes, and a non-zero current reading and rate of buildup appear on the hand-held controller display. The sulfuric acid dew-point temperature is measured at the sensor tip temperature at which the current reading is 100 micro amperes (μA) and the rate of buildup is near zero.

## *2.3 Dew-Point Temperature Measurement Technique*

Because the dew-point meter employed was designed specifically for the detection of sulfuric acid dew point, we found it necessary to modify its use for our determination of ABS formation temperature. In particular, we could not use the 100 μA current condition as a reliable requirement for reproducible measurements. Extending from the idea of a thin film of condensate forming on the glass tip and producing a steady predetermined current reading, we introduce a

concept for identifying ABS formation temperature range. The steps taken are summarized as follows:

1. A preliminary temperature range was first assumed by observing the Matsuda and Radian ABS formation temperature curves at specific reaction concentrations.
2. The probe temperature was held at each temperature for approximately 20 minutes for the determination of an increasing or decreasing current reading.
3. The maximum and minimum temperatures of the range were tested first and then the midpoint temperature. The result of either condensation or evaporation indicates which midpoint temperature should be tested next.
4. Repeating the previous steps created a narrower and narrower ABS dew formation temperature range for each reactant concentration combination.

A real-time plot of the meter temperature and current reading is shown in Figure A-3 to illustrate our method. With this approach, an increase in current indicates ABS condensation, and a decrease indicates ABS evaporation. The new ABS dew-point temperature range lies between the highest condensation and lowest evaporation temperatures. We also identify the temperature at which there is neither condensation nor evaporation as the actual dew-point condition. However, because detecting slow current increases and decreases is difficult, we included the range as well.

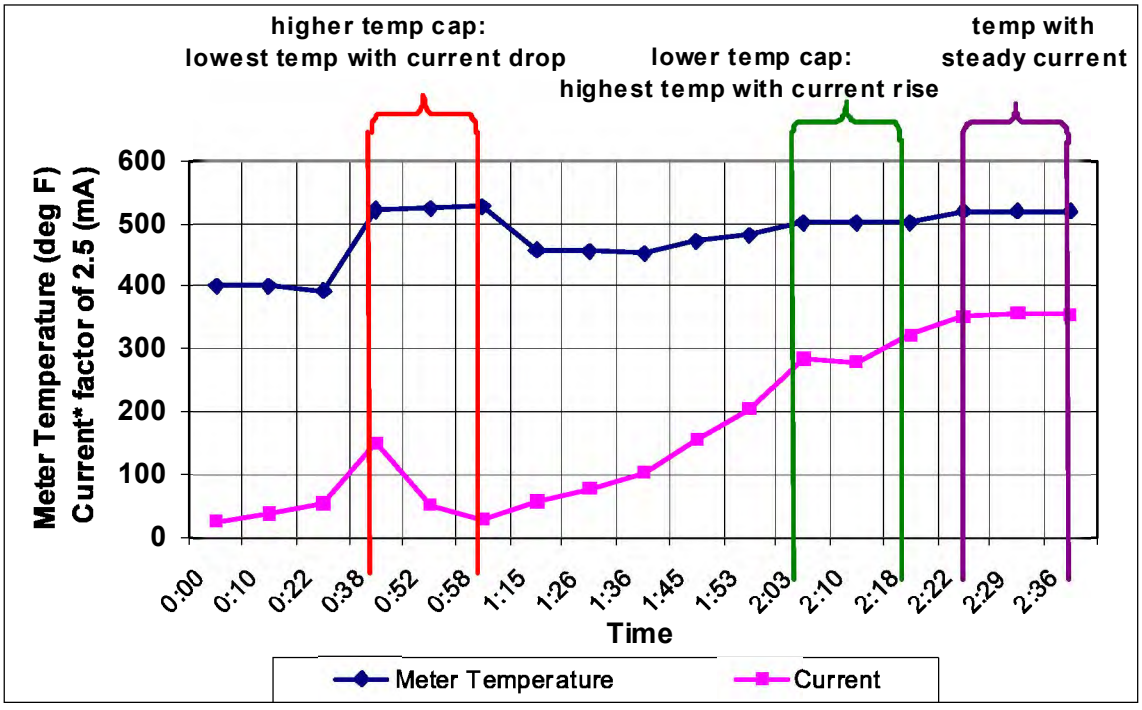


**Figure A-3**
**Meter Temperature and Current vs. Time**

## 3 Results and Discussion

The ABS formation temperature range described above was determined at five reactant concentration combinations, as shown in Table A-2, over a range of the product of $H_2SO_4$ x $NH_3$ of 392 to 6371. For each test condition, the $SO_3$ and $NH_3$ concentrations were measured using the techniques described previously, along with the dew-point temperatures. Our experimental temperature ranges are plotted along with results from Matsuda et al. and Radian for comparison within the reactant concentration range typical of air preheater conditions. For each reactant combination, three temperatures are marked:

- The lower temperature at which an increase in current is recorded ⇒ left x error bar
- The temperature at which the sensor current appears steady ⇒ data point
- The high temperature at which a decrease in current is recorded ⇒ right x error bar

**Table A-2**
**Test Conditions: $H_2SO_4$ and $NH_3$ Concentrations**

| Test | $SO_3$ ppm | $NH_3$ ppm | $SO_3$ * $NH_3$ ppm^2 |
|---|---|---|---|
| 1 | 39 | 163 | 6371 |
| 2 | 11 | 43 | 489 |
| 3 | 19 | 21 | 392 |
| 4 | 18 | 182 | 3362 |
| 5 | 21 | 31 | 661 |

The results are shown in Figure A-4. Note that the range in the three temperatures defined above for each test was only about 10°F.

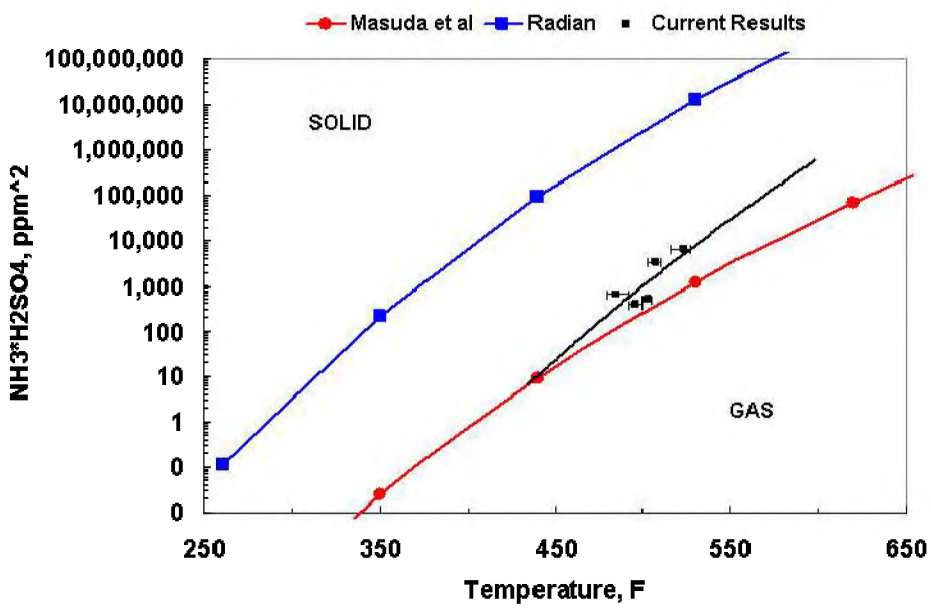


**Figure A-4**
**Reactant Concentration vs. ABS Formation Temperature**

Our current results are between the Radian and Matsuda et al. curves, tending more toward the Matsuda et al. curve than the Radian curve. The left x error bar on each data point indicates the highest condensation temperature, while the right one indicates the lowest evaporation temperature. The error in reactant concentrations are smaller than the size of the data point plotted on the logarithm scale. We believe that the resulting curve is lower than that of Matsuda's likely as a result of the experimental procedure used in that study. However, there are several other factors that warrant consideration in the current study. Also, the slope of the line differs from the Matsuda et al. results.

One reason for the noticeable difference is that Radian results assume ideal clean gas conditions with no condensation nuclei to assist the process. Although we operate a natural-gas-burning combustor, the combustor has been used for various other research projects. Several of these include the injection of fly ash and catalyst powder. Impurities present in our combustor inputs or any of residuals mentioned may serve as nuclei for heterogenous nucleation, causing the ABS to condense sooner than it would otherwise and, thus, effectively raising the ABS formation temperature detected.

Second, there is a boundary layer between the gas approaching the sensor and the surface of the sensor. Condensation could start to occur in the boundary layer at a higher temperature than the sensor temperature. In this case, the higher temperature noted in the current procedure may be a better indication of the ABS dew point. Again, this requires further study.

In reality, most air preheater practices tend to use a formation temperature close to the Radian curve, while catalyst manufacturers tend to use the Matsuda et al. curve to set minimum SCR operation temperatures. The current results suggest that the catalyst vendors may be conservative in setting the minimum operating temperature, whereas with air preheaters, the ABS may be forming in a different part of the air preheater than predicted by the Radian curve.

# 4 Future Work

Although the experimental data have provided new ABS formation temperature results, these values should be viewed as preliminary. We need to verify our reactant concentrations and understand the role of thermal gradients in the flow (particularly for relevance to air preheater channels). Further testing will involve a test in the field and a laboratory air preheater channel model for detailed measurements of ABS formation. Experiments varying the gas velocity and temperature will be conducted in attempts to investigate boundary layer effects.

## *4.1 Summary*

ABS dew-point temperature was measured using a dew-point meter with a modified measurement technique. The result within the reactant concentrations range of 300 ~ 1500 $ppm^2$ were compared to two other existing curves. The new ABS formation temperature curve is approximately 50°F lower than that reported by Matsuda et al. and almost 100°F higher than that reported by Radian.

## 5 Acknowledgments

This joint project is supported by the University of California, Irvine, Electric Power Research Institute, and Fossil Energy Research Corporation. Also, special thanks go to Q. Qader and K. Anderson from FERCO for their help.

## 6 References

1. K. Johnson and J. Burke, "An Investigation of Ammonium Sulfate/Bisulfate Formation and Deposition in Air Preheaters," Radian Corporation, 1980.
2. Matsuda et al. Industrial and Engineering Chemistry Product Research and Development, 21(1), pp. 48–52 (1982).
3. Kelley et al. United States Bureau of Mines, Technical Paper No 688, pp. 66–69, 1946.
4. W. D. Scott and F. C. R. Cattell. *Atmospheric Environment*, 13, pp. 307–317 (1979).
5. C. Galloway, G. Blythe, and R. Rhudy. *Proceedings of the Mega Symposium* (2001).
6. G. C. Quartucy, D. P. Teixeira, L. J. Muzio, and T. A. Montgomery, Joint EPRI/EPA Symposium on Stationary $NO_x$ Control, (1993).
7. S. Gordon and B. McBride. National Technology Transfer Center, Document ID 19720000717; Accession ID 72B10718, 1972.
8. Breen et al. DOE Environmental Control Conference, Document ID 19720000717; Accession ID 72B10718, 2006.

# B
# CFD MODELING SUMMARY (EPRI)

EPRI | ELECTRIC POWER RESEARCH INSTITUTE

## Memorandum

Date 5/31/2007

TO: Jeff Stallings

FROM: Alex Jimenez

SUBJECT: Project Update – Numerical Simulation of an Air Preheater Model

### Executive Summary

The overall objective of this project was to develop a numerical model subroutine in order to model a regenerative air preheater (APH). The model was developed using the commercial computational fluid dynamics (CFD) code FLUENT along with custom-designed subroutines, termed *user-defined functions* or UDFs, to account for the thermal simulation. The UDF was designed to model heat transfer rates between hot flue gas and cold air sides and the interaction with the rotating metal baskets. This functionality was accomplished by using bulk flow heat transfer correlations and algorithms previously developed for EPRI's Rotational Preheater Metal Temperature (RPHMT) air heater model. Three different methods to simulate a full air heater were attempted; however, none of the models provided a satisfactory solution. EPRI with support from ANSYS/Fluent will continue to investigate options for developing a full-scale model of the air heater.

A more successful approach was to model only a single air flow path or basket channel. The primary objective of this simplified approach was to predict fluid and thermodynamic effects inside a single air heater channel while accounting for the air space that exists between the various basket layers of an APH. In order to conduct the single-channel simulation, wall temperatures and inlet boundary conditions were obtained from a case study solved with the RPHMT code. The CFD-predicted flue gas temperatures from this single-channel model were 12.6°F (7 K) higher than those predicted by the RPHMT model. However, these results were based on a different inlet open area and shape than the bulk conditions assumed by the RPHMT model.

EPRI will continue to work to obtain additional field data to complete and validate a single-channel model. The proposed additional modeling work is summarized below:

- Model a group of channels (at least nine) to capture flue gas mixing that may occur in the space between layers.

- Model channels of specific geometry typical of APH baskets, such as notched flat inlets.
- Incorporate ash particle injections coupled with the continuous phase flow solution, if proper particle interaction information can be found, This information includes ash rebound coefficient information and ash particle size distribution.
- Investigate the option of modeling ABS formation and deposition using other simulation tools that incorporate species formation and condensation, particle-particle dynamics, and droplet formation.
- Work will continue toward development of a full-scale APH.

## Introduction and Background

EPRI developed a modeling tool to predict rotating metal temperatures of regenerative air preheaters (APHs) called the Rotational Preheater Metal Temperature (RPHMT). The code uses information from APH geometry and operating conditions, such as inlet temperatures, gas flow rates, and APH speed, to predict gas temperatures and APH thermal performance. EPRI's RPHMT code is a two-dimensional numerical model that predicts temperatures in the axial (gas flow direction) and peripheral direction at a specified radial distance. The RPHMT model provides the ability to quickly predict heat transfer effects due to changes in operating parameters, such as gas side temperatures or rotational speed. Other applications include the effects on metal temperature distribution due to design changes, such as the removal of metal elements or the change of element material or design geometry.

In addition to fluid side and metal temperatures, EPRI's APH model predicts a location where ammonium bisulfate (ABS) is most likely to form and deposit based on dew-point temperature calculations that include $NH_3$ and $SO_3$, concentrations.

In the present effort, it was desired to expand the two-dimensional approach of the existing EPRI APH model into a three-dimensional CFD model of a complete air heater. The objective of this model is to predict fluid and metal temperatures and to account for the impact of intermediate spaces between the various rotational basket layers. When completed, the three-dimensional APH would be coupled with species mixing and thermal effects to (1) map locations within the APH baskets where ammonia bisulfate (ABS) may form under a given set of conditions, and (2) investigate design adjustments to optimize heat transfer and reduce the chance of ABS deposition. These design adjustments could include:

- Number of basket layers
- Space between layers
- Layer length
- Metal physical properties
- Basket porosity
- Rotational speeds
- Channel geometry type

Other anticipated flue gas variations are:

- Changes to fluid side velocity, temperature, and species

- Simulation of non-uniform inlet profiles

## Approach

### *Full-Scale APH Model*

The three-dimensional model incorporated the domain of both air and gas sides. Thus the model was developed to provide air side temperatures as well as gas side temperatures. The metal matrix of the air heater was simulated using a number of approaches, but none included a complete geometry of the metal baskets. The model had two inlets and two outlets. During this effort, dimensions and variables for a three-layer APH from the EPRI RPHMT model were used for development. The model required a user-defined subroutine to simulate the heat transfer between the air/gas and the metal baskets. ANSYS/Fluent was the contractor who developed the subroutine and provided support to the EPRI team. Figures B-1 and B-2 present contour plots of the initial metal matrix and fluid side temperature predictions from the three-dimensional model.

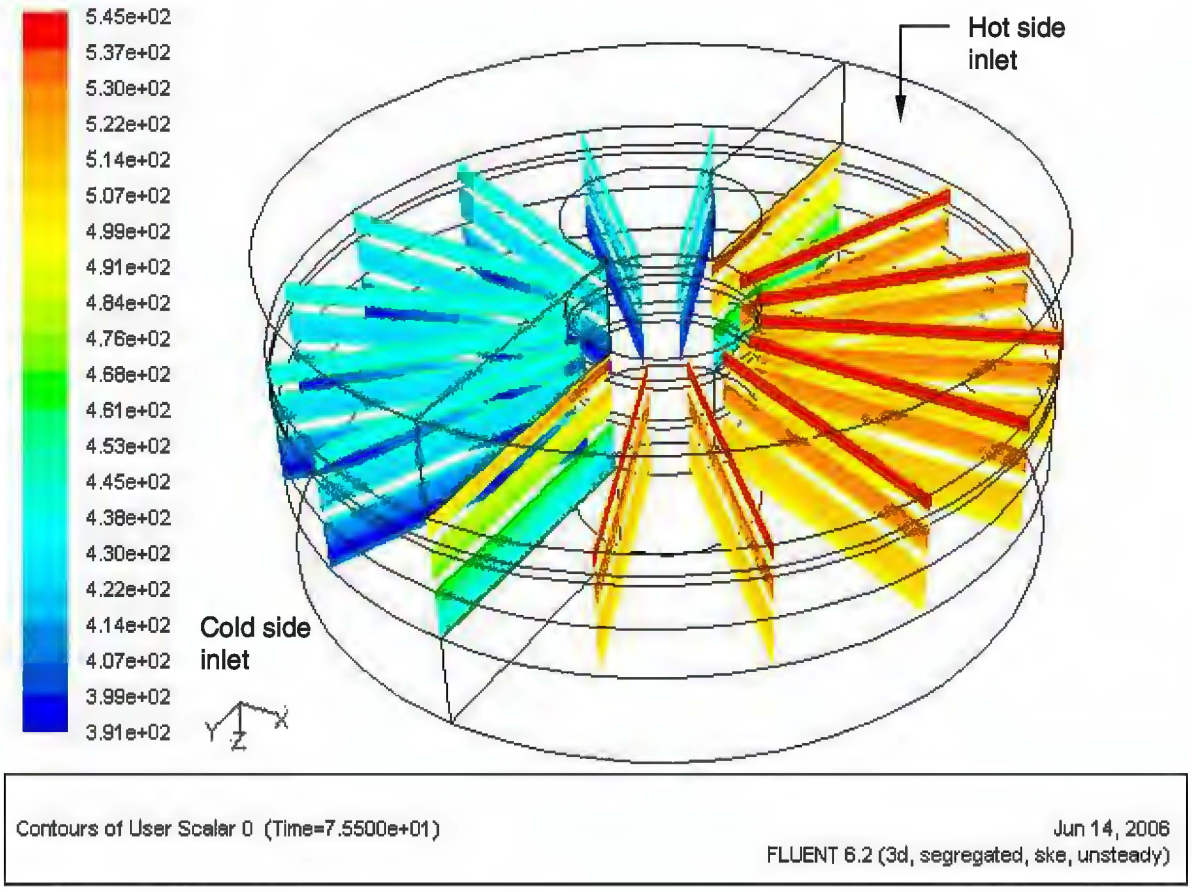


**Figure B-1**
**Preliminary Results – Metal Temperatures**

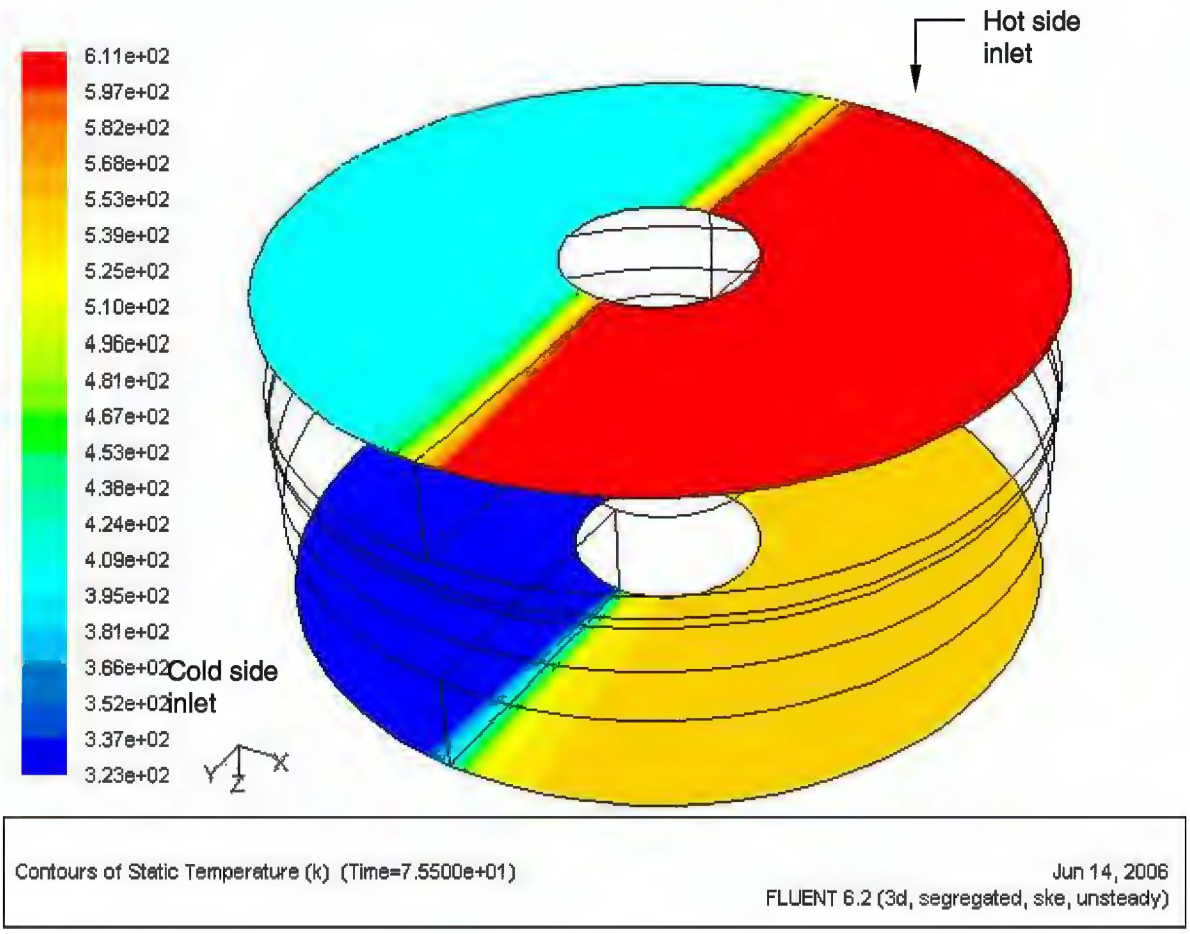


**Figure B-2**
**Preliminary Results – Gas Side Temperatures**

### *Single-Channel Model*

In addition to the full-scale APH model, a single APH channel was modeled. The geometry includes three channels to represent the hot, intermediate, and cold layers. As illustrated in Figure B-3, flue gas enters at the inlet located 10 inches above the hot layer; passes through the hot, intermediate, and cold layers consecutively; and exits at the outlet 10 inches below the cold layer.

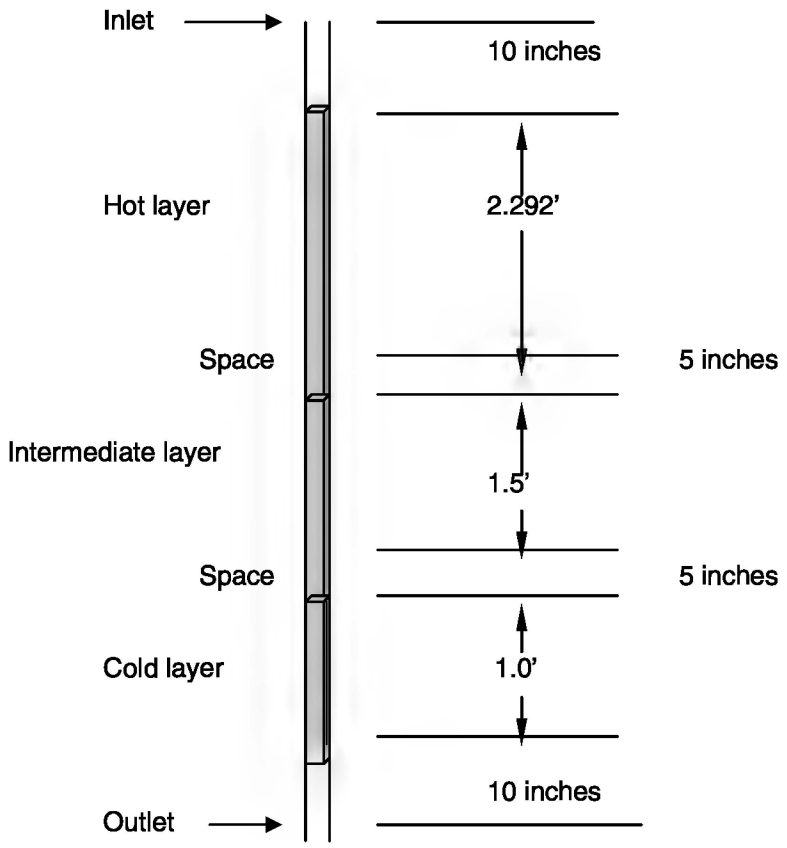


**Figure B-3**
**Single-Channel Dimensions**

The sections between layers were modeled using planes of symmetry in order to simulate an isotropic condition. This functionality creates a mirror plane at the selected surface and assumes identical conditions on both sides of the face. This approach assumes that fluid coming out of one layer flows directly into the next layer. The sections between layers were modeled using the standard k-e turbulence model, and the channel sections were modeled as laminar flow zones.

Inlet boundary conditions are listed in Table B-1. The channel open area is 0.234 in2 (1.5E-4 m2). Using total mass flow to open area ratio, a total of 13.3 lbs/hr (0.00168 Kg/s) was estimated at the inlet. This number is based on a total air heater flow rate of 2023 klbs/hr.

**Table B-1**
**Channel Boundary Conditions**

| | | |
|---|---|---|
| Inlet Area | 0.00015081 | $m^2$ (0.23375 $in^2$) |
| Hydraulic diameter | 0.00768 | m (0.30236 in) |
| Flue gas temperature | 611 | K (640°F) |
| Mass flow | 0.00168 | Kg/sec (13.14 lb/hr) |
| Average Re inside channel | 2750 | |
| $NH_3$ | 5 | ppm |
| $SO_3$ | 8 | ppm |

Tables B-2, B-3, and B-4 present minimum and maximum metal matrix temperature as a function of length. The temperatures were extracted from the RPHMT and were used in the CFD model as wall initial boundary conditions. Additional metal properties are listed in Table B-5.

**Table B-2**
**Hot Layer – Metal Temperatures**

| Layer Distance Feet | Minimum Temperature Fahrenheit | Maximum Temperature Fahrenheit |
|---|---|---|
| 4.724 | 590.15 | 613.48 |
| 4.515 | 577.84 | 600.74 |
| 4.307 | 566.48 | 589.96 |
| 4.098 | 555.15 | 579.4 |
| 3.890 | 543.57 | 568.65 |
| 3.682 | 531.59 | 557.57 |
| 3.473 | 519.15 | 546.07 |
| 3.265 | 506.14 | 534.09 |
| 3.057 | 492.32 | 521.45 |
| 2.848 | 477.01 | 507.68 |
| 2.640 | 457.36 | 492.03 |

**Table B-3**
**Intermediate Layer – Metal Temperatures**

| Layer Distance Feet | Minimum Temperature Fahrenheit | Maximum Temperature Fahrenheit |
|---|---|---|
| 2.468 | 458.09 | 495.34 |
| 2.331 | 443.11 | 478.4 |
| 2.195 | 430.65 | 466.02 |
| 2.058 | 419 | 454.84 |
| 1.922 | 407.46 | 443.93 |
| 1.786 | 395.76 | 432.97 |
| 1.649 | 383.76 | 421.79 |
| 1.513 | 371.23 | 410.23 |
| 1.377 | 357.75 | 397.97 |
| 1.240 | 342.03 | 384.2 |
| 1.104 | 320.02 | 368.5 |

**Table B-4**
**Cold Side Layer – Metal Temperatures**

| Layer Distance Feet | Minimum Temperature Fahrenheit | Maximum Temperature Fahrenheit |
|---|---|---|
| 1.000 | 336.61 | 389.62 |
| 0.929 | 323.63 | 371.1 |
| 0.857 | 312.36 | 358.63 |
| 0.786 | 302.79 | 348.86 |
| 0.714 | 294.09 | 340.26 |
| 0.643 | 285.75 | 332.18 |
| 0.571 | 277.51 | 324.3 |
| 0.500 | 269.22 | 316.46 |
| 0.429 | 260.72 | 308.52 |
| 0.357 | 251.81 | 300.31 |
| 0.286 | 242.08 | 291.53 |
| 0.214 | 230.69 | 281.59 |
| 0.143 | 215.64 | 269.71 |
| 0.071 | 193.74 | 257.33 |
| 0.000 | 193.74 | 257.33 |

**Table B-5**
**Metal Physical Properties**

| Property | Value | Units |
|---|---|---|
| Density | 7737 | $Kg/m^3$ |
| Cp | 465 | J/Kg-K |
| Thermal conductivity | 48 | W/m-K |
| Shear condition | none | |
| Roughness | 0.5 | |

## Results

### *EPRI's Rotating Preheater Metal Temperature (RPHMT) Results*

Boundary conditions provided in Tables B-1 and B-2 were used to set up and run EPRI's RPHMT model. Figure B-5 shows the locations along the APH hot side where minimum and maximum flue gas and metal basket temperatures occur. The graph in Figure B-6 presents estimated minimum and maximum metal and fluid temperatures along the axial length of the APH for the hot side section. The curve starts at the cold end layer and ends at the hot end layer. The radial distance is 16 feet from the center of the APH.

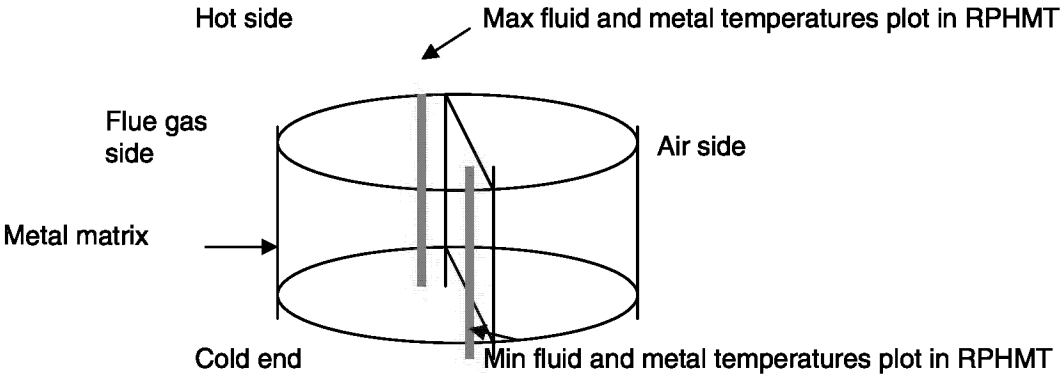


**Figure B-5**
**APH Indicating Lines Plot in RPHMT**

As discussed previously, in addition to fluid and metal temperatures, the RPHMT also predicts a critical zone where ABS is most likely to deposit. This zone falls between the maximum flue gas temperature and the minimum metal temperature, and between the ABS melting and formation temperature curves (see the circled zone in Figure B-6).

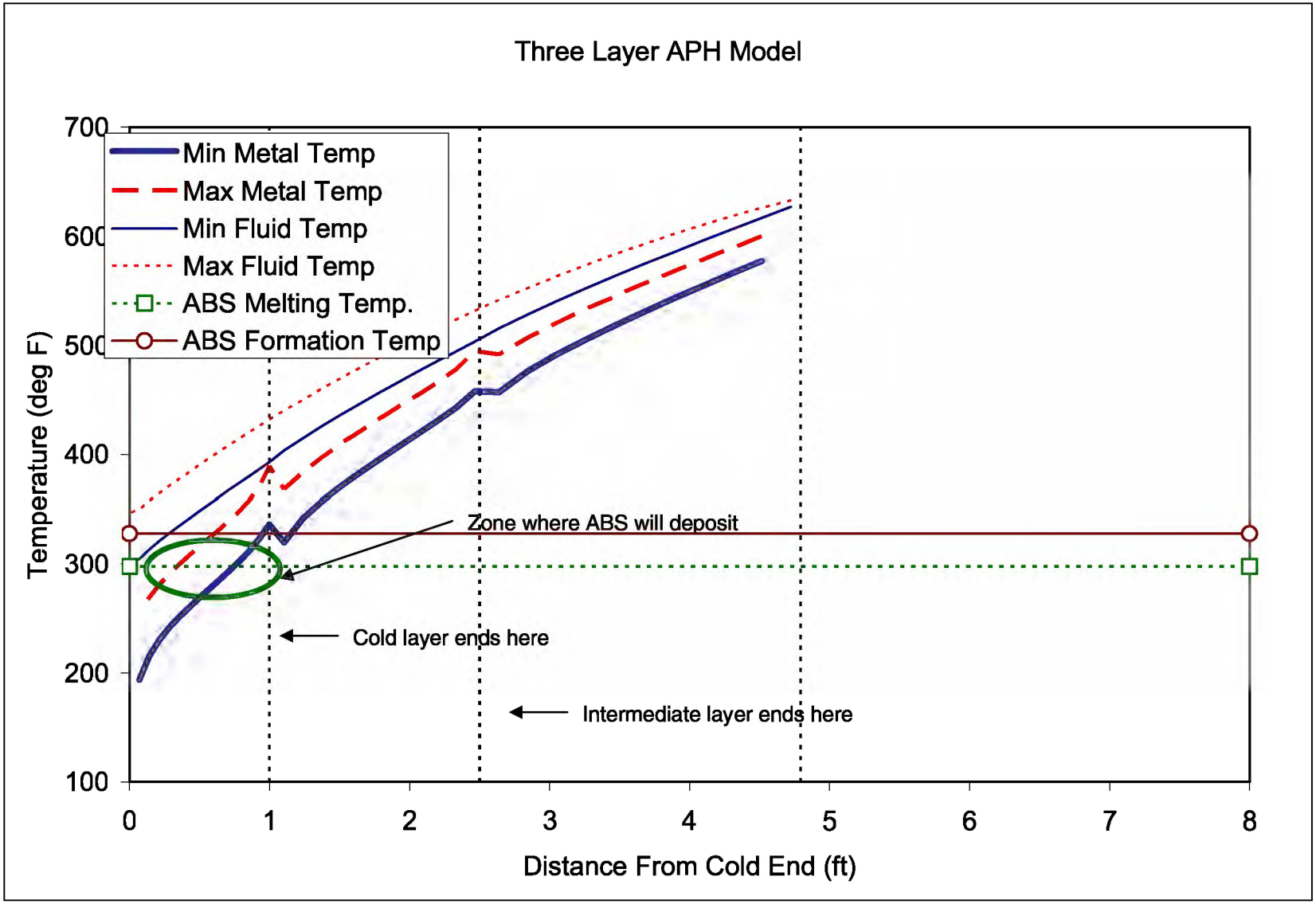


**Figure B-6**
**Baseline RPHMT Results (r = 16 ft)**

### *Full-Scale APH*

The following information describes the different methods that were tried to simulate the flow and heat transfer using a full three-dimensional model of a regenerative APH.

**1. Moving Reference Frame (MRF) Approach**

The metal matrix was modeled using a porous rotating zone. The resistance that the metal basket offers to the fluid was modeled by enabling inertial and viscous resistance coefficients. To model thermal nonequilibrium between the basket and the fluid, a transport equation was solved representing the energy of the metal basket. This was solved using the user-defined scalar approach (UDS) in the FLUENT code. The metal basket energy equation that needs to be solved is

$$\partial/\partial t\,(\rho H) + \nabla \bullet (v\rho H) = \nabla \bullet (k\nabla T) + S_H \qquad \textbf{Equation B-1}$$

Where $\rho$ is the density of the solid, k is the conductivity, $S_H$ is the volumetric heat source, and H is the sensible enthalpy and is given by

$$\int_{T_{ref}}^{T} C_p dT \qquad \textbf{Equation B-2}$$

Where $T_{ref}$ is 298.15 K, and T is temperature of the solid. The second term on the left side of equation B-1 represents convective energy transfer due to rotational or translational motion of the solid. v is computed from the motion specified for the solid zone. The terms on the right side are the heat flux due to conduction and volumetric heat source within the solid.

The FLUENT code has the option to specify the fluid zone as laminar. This option disables the turbulence production, but transports the turbulence quantities. The superficial velocity within the porous region is defined as

$$v_{\text{superficial}} = \gamma v_{\text{physical}}$$

Where $\gamma$ is the porosity of the media defined as the ratio of the volume occupied by the fluid to the total volume. Using the physical velocity formulation and assuming a general scalar $\phi$, the governing transport equation in an isotropic porous medium has the following form:

$$\frac{\partial \rho\phi}{\partial t} + \frac{\partial}{\partial x_i}\left(\rho u_{i\phi} - \Gamma \frac{\partial \phi}{\partial xi}\right) = S_\phi$$

Where $\rho$ is the density of fluid. Here, the UDS can represent the enthalpy of the basket. The solid basket temperature field was obtained from the UDS field by

$$T_{solid} = \frac{\rho_{fluid}\, x\, \phi x (1 - porosity)}{\rho_{solid}\, x C_{\rho_{solid}}} + T_{ref}$$

(This is assuming constant *Cp* for solid.)

The above given solid temperature formulation was calculated using a user-defined function (UDF) and stored into user-defined memory at each grid location. To achieve heat transfer between fluid and solid, energy source terms were calculated based on the difference between the temperature of the fluid and the temperature of the solid calculated above. The heat transfer coefficient was obtained from the empirical correlations that were provided by EPRI. The energy source term was applied to the energy equation in the fluid region; an equal and opposite source term was applied to the UDS equation, which represents the energy equation in the solid basket.

To ensure that the UDS formulation is correct, a test case was run. Here, a closed cylinder with a MRF formulation was used (see Figure B-7). Initially, a flow field was established that was essentially the solid rotation flow field (see Figure B-8). In one half of the cylinder, energy was assigned a source of value 1 $W/m^3$, and in the other, a sink of -1 $W/m^3$. (0.0966 $Btu/hr\text{-}ft^3$)In the same regions, a UDS was also assigned source and sink values of 1 and -1. The resulting fields of temperature of fluid and temperature from the UDS were compared (Figures B-9 and B-10). The comparisons showed that the temperature from the UDS formulation matches with that of the fluid very well.

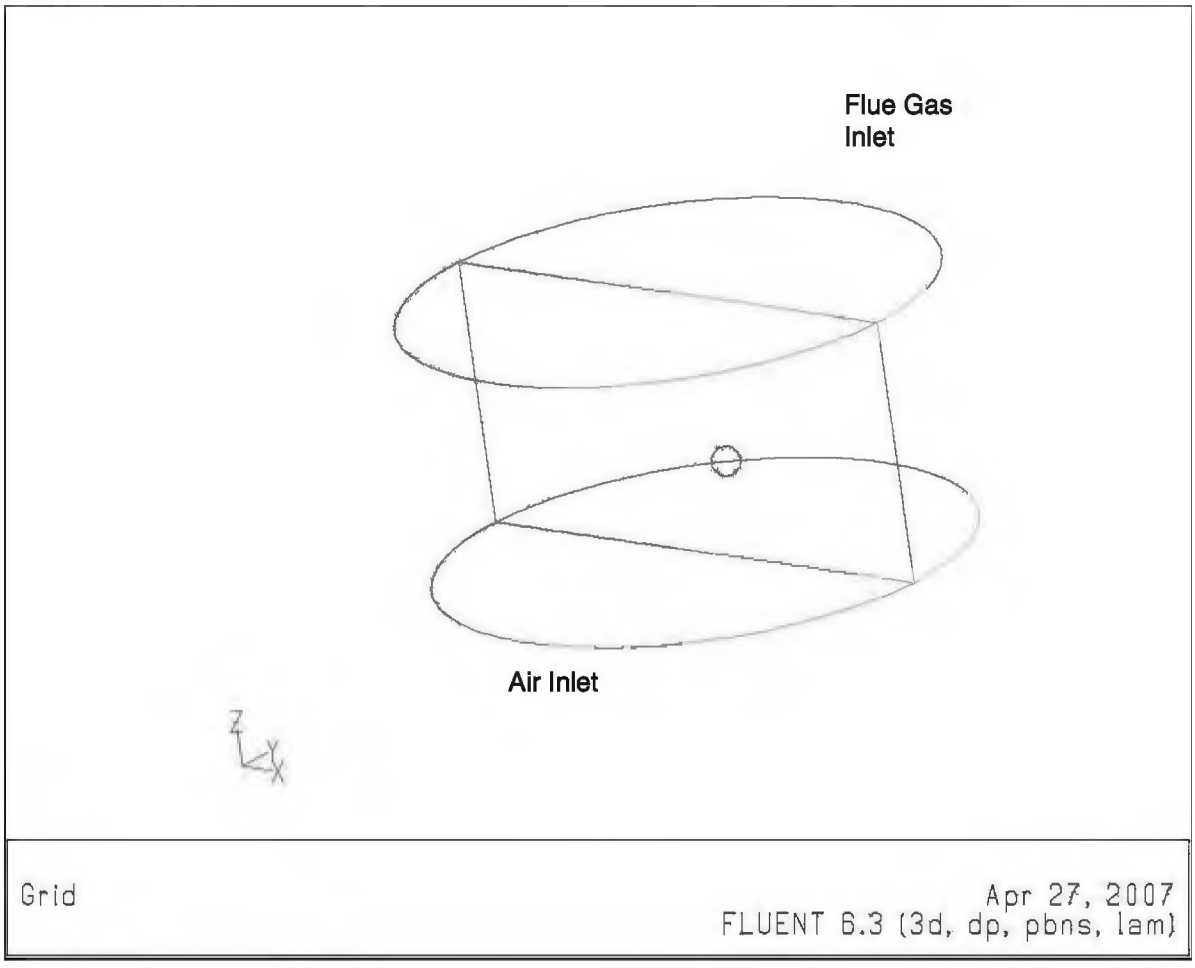


**Figure B-7**
**Model Geometry**

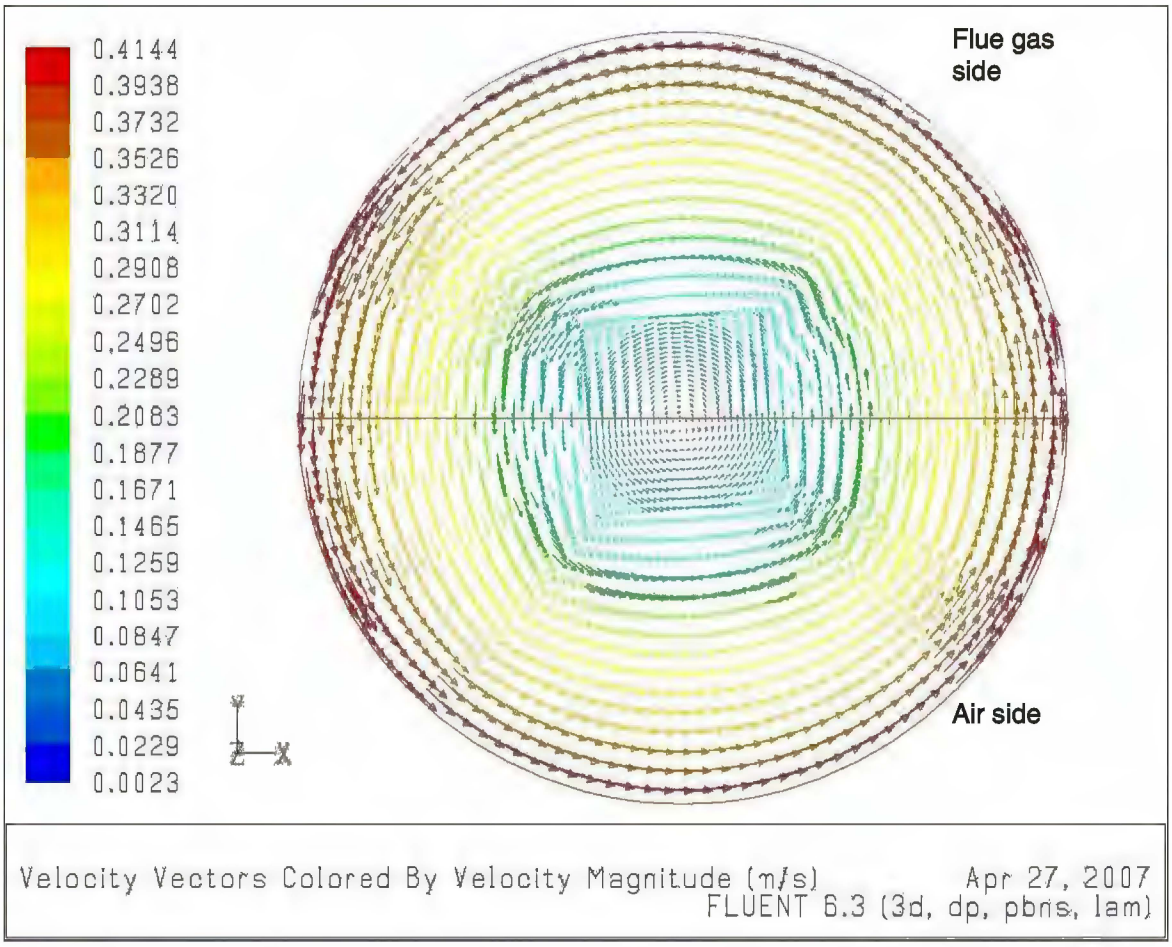


**Figure B-8**
**Velocity Vectors (Top View)**

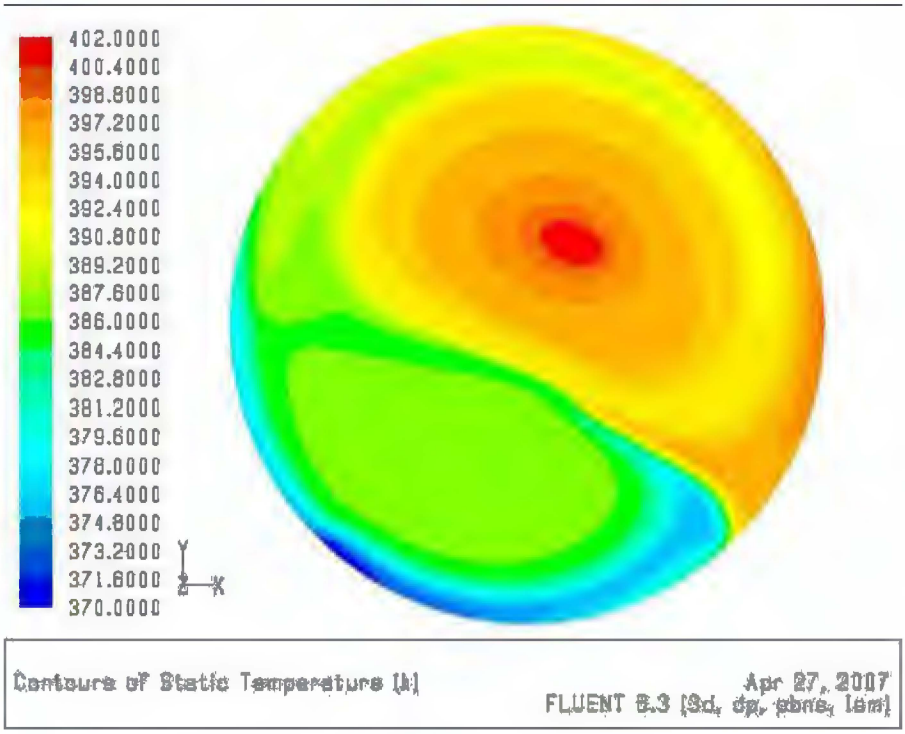


**Figure B-9**
**Fluid Temperature (Top View)**

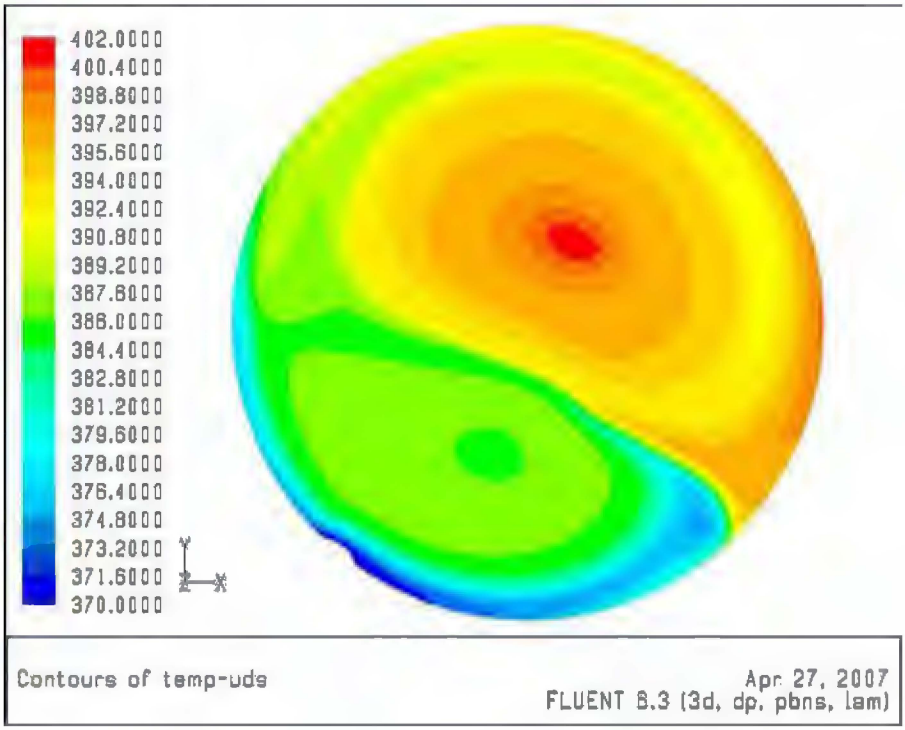


**Figure B-10**
**Metal Temperature (Top View)**

As can be seen from the UDS equation above, the convective flux term in the UDS equation needs the velocity field to be that of the solid rotation. In case of flow through the APH, the fluid velocity field is very different from the solid rotation velocity field. Therefore, it was necessary

to provide the appropriate flux term by writing a customized flux function. However, a suitable function was not found.

**2. Sliding Mesh Approach**

The correlations used to develop the UDF subroutine produced very high "h" values, which would cause unrealistic temperatures to be predicted. After spending a considerable amount of time debugging the UDS flux function approach, a different approach was attempted in order to predict heat transfer between the baskets and the fluid. The idea was to use the unsteady solver to resolve the transient behavior of the rotating heater section using a sliding mesh model. A new test case was created, and the same flow conditions were simulated except that a constant heat transfer coefficient was assumed. This approach, however, required a very small time step to run and, consequently, would need several converged time steps in order to simulate one air heater revolution (~60 seconds) This approach did not yield a satisfactory solution either.

**3. Multiphase Model Approach**

In the multiphase approach, the metal basket was treated as the secondary phase or phase 2 and fluid (air or flue gas) was treated as the primary phase or phase 1. The heat transfer between the phases was modeled using a heat exchange UDF. The heater section was modeled as porous medium, and the heat exchange UDF used a constant "h" as used in the sliding mesh approach. The case was run under a steady-state assumption. There was no inlet or outlet for the granular phase. In order to maintain the granular phase in the domain, the required volume fraction of granular phase was patched or frozen in the heater section, and the volume of fluid (VOF) equation is turned off. Also to ensure the rotation of the granular phase, a fixed velocity option was used to superimpose a flow profile. Although several variations were tested, this approach did not yield results to indicate that an energy balance was satisfied.

### *Single-Channel Model Results*

CFD-predicted temperature profiles are plotted in Figure B-11. Minimum and maximum metal matrix temperatures are the same as the RPHMT results previously presented in Figure B-6. However, this approach models the spaces between layers.

CFD and RPHMT temperature results are summarized in Table B-6. Overall, CFD fluid temperatures at the outlet are 12.6°F (7 K) higher than the RPHMT results. Note that these results represent a preliminary estimate and are based on assumed channel cross-sectional area.

**Table B-6**
**RPHMT and CFD Temperatures at the Cold Layer Outlet (Kelvins)**

| Minimum Temperatures (°F [K]) | | | Maximum Temperatures (°F [K]) | | |
|---|---|---|---|---|---|
| **RPHMT** | **CFD** | **Diff.** | **RPHMT** | **CFD** | **Diff.** |
| 300 (422) | 312 (429) | 12.6 (7) | 347 (448) | 359.6 (455) | 12.6 (7) |

The RPHMT has the option to select between notched flat, notched undulated (corrugated), or double undulated channels; however, no channel dimensions are required. Each of the element types uses different empirical correlations to estimate a Nusselt Number (Nu) inside the channel.

The CFD model uses a rectangular inlet with dimension of 0.17 in (.0043 m) by 1.375 in (0.0349 m) for a total open area of 0.234 $in^2$ (1.51 $m^2$). In addition, the RPHMT does not include mixing effects between baskets, but the CFD model includes the space between baskets.

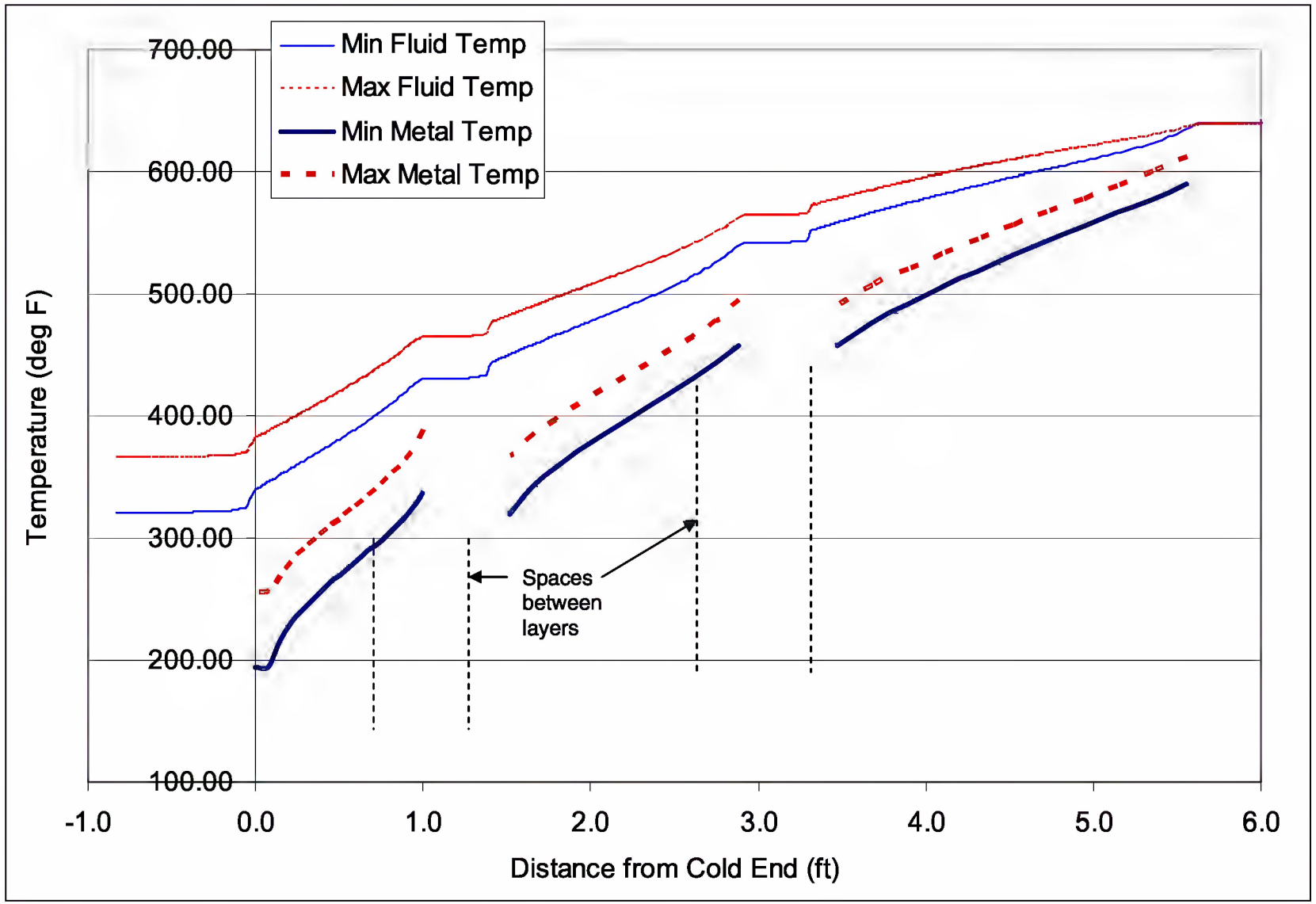


**Figure B-11**
**CFD Single-Channel Results**

Figure B-12 below depicts a temperature contour plot across the channel at the hot layer. The model predicted a temperature gradient of 45°F (25 K) from the wall to the center of the channel.

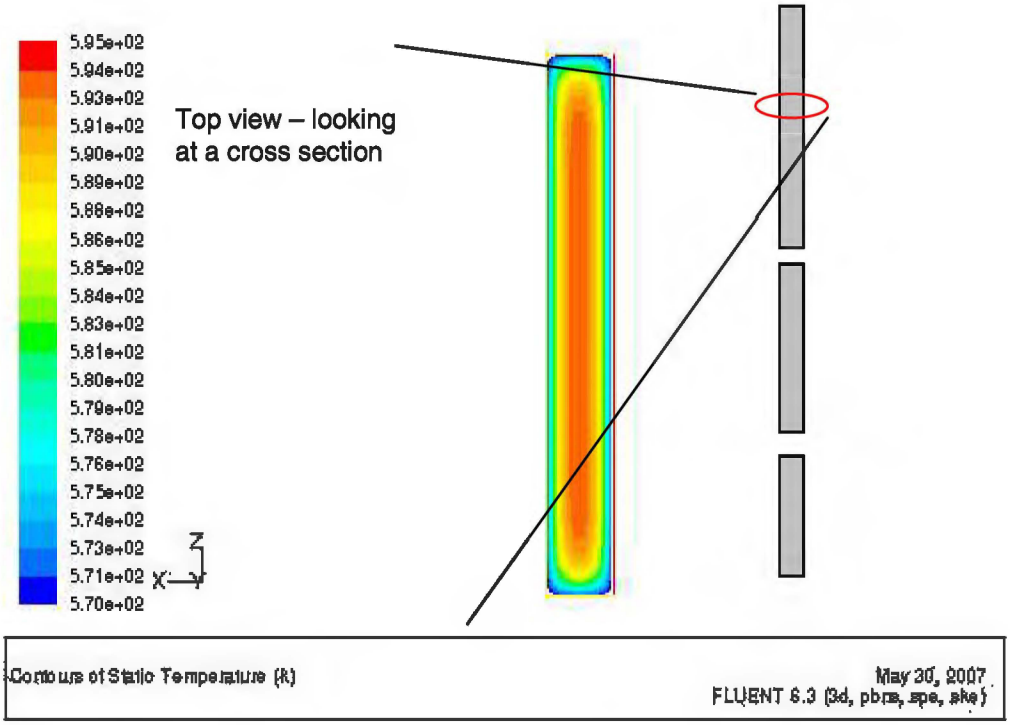


**Figure B-12**
**Fluid Temperature Contour Plots Inside the Channels (Cross Section)**

## Conclusion and Future Work

### *Conclusions*

The regenerative APH full-scale three-dimensional simulation was attempted using three different methods. Although some results indicated heat transfer and metal temperature predictions, none of the three methods provided satisfactory solutions. The algorithms derived from the RPHMT code, which are based on global heat transfer correlations of the air heater, did not yield satisfactory results with the volumetric cell approach used by the CFD code.

Flue gas through a single channel was also simulated using FLUENT. The overall objective was to predict thermodynamics and fluid dynamics effects inside the channel and between layers. This approach seems to provide a satisfactory approach to providing more detailed flow and thermal information. Once the model is further developed, the results will be applied by the project team to investigate the phenomena that may impact ABS formation and deposition inside APHs.

### *Proposed Future Work*

Based on the knowledge obtained from the concurrent laboratory work, an assessment of the applicability of the CFD approach should be conducted. In this past effort, the objectives of the

CFD models were to enhance the capability of the existing approach to provide more information about the possible temperature profiles that may occur inside the air heater.

## Proposed Work Includes:

### Full-Scale APH

- Further development is required to create a model to simulate a full-scale regenerative APH. This is an issue that should be resolved and that would become beneficial from a global perspective of the air heater operation.

### Single-Channel APH

- Efforts will continue to model a group of channels as opposed to only one channel. In the previous model, planes of symmetry were used between layers. This approach assumed that the flow coming out of one layer went into the next one. Modeling a group of channels will eliminate the need for planes of symmetry; therefore, this option will explore additional mixing effects between layers (for example, tracking flow inside the highlighted channel in Figure B-13).

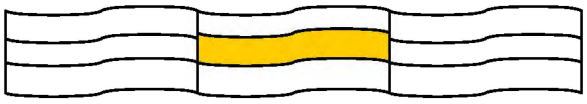

**Figure B-13**
**Proposed Group of Channels – Top View**

- Model a notched-flat channel as opposed to a rectangle, and confirm inlet boundary conditions (flow area and mass flow).
- Simulate the flow of ash in the air heater by including a discrete second phase (coupled with the continuous phase flow solution.
- Identify literature information or laboratory information for modification of wall surface conditions (roughness) into the modeling effort.
- Investigate ABS formation and deposition using FLUENT's species transport with the reaction mechanism option. In addition, the application of a fine particulate model to account for particle formation, growth, transport, and deposition is also being considered.

**Export Control Restrictions**

Access to and use of EPRI Intellectual Property is granted with the specific understanding and requirement that responsibility for ensuring full compliance with all applicable U.S. and foreign export laws and regulations is being undertaken by you and your company. This includes an obligation to ensure that any individual receiving access hereunder who is not a U.S. citizen or permanent U.S. resident is permitted access under applicable U.S. and foreign export laws and regulations. In the event you are uncertain whether you or your company may lawfully obtain access to this EPRI Intellectual Property, you acknowledge that it is your obligation to consult with your company's legal counsel to determine whether this access is lawful. Although EPRI may make available on a case-by-case basis an informal assessment of the applicable U.S. export classification for specific EPRI Intellectual Property, you and your company acknowledge that this assessment is solely for informational purposes and not for reliance purposes. You and your company acknowledge that it is still the obligation of you and your company to make your own assessment of the applicable U.S. export classification and ensure compliance accordingly. You and your company understand and acknowledge your obligations to make a prompt report to EPRI and the appropriate authorities regarding any access to or use of EPRI Intellectual Property hereunder that may be in violation of applicable U.S. or foreign export laws or regulations.

**The Electric Power Research Institute (EPRI),** with major locations in Palo Alto, California; Charlotte, North Carolina; and Knoxville, Tennessee, was established in 1973 as an independent, nonprofit center for public interest energy and environmental research. EPRI brings together members, participants, the Institute's scientists and engineers, and other leading experts to work collaboratively on solutions to the challenges of electric power. These solutions span nearly every area of electricity generation, delivery, and use, including health, safety, and environment. EPRI's members represent over 90% of the electricity generated in the United States. International participation represents nearly 15% of EPRI's total research, development, and demonstration program.

Together…Shaping the Future of Electricity



*Printed on recycled paper in the United States of America*

1016164

**Electric Power Research Institute**
3420 Hillview Avenue, Palo Alto, California 94304-1338 • PO Box 10412, Palo Alto, California 94303-0813 • USA
800.313.3774 • 650.855.2121 • askepri@epri.com • www.epri.com